ISSN 2096-7071 (Print)
ISSN 2096-3101 (Online)
CN 10-1629/R1

CHINA CDC WEEKLY

Vol. 6 No. 33 Aug. 16, 2024

中国疾病预防控制中心周报

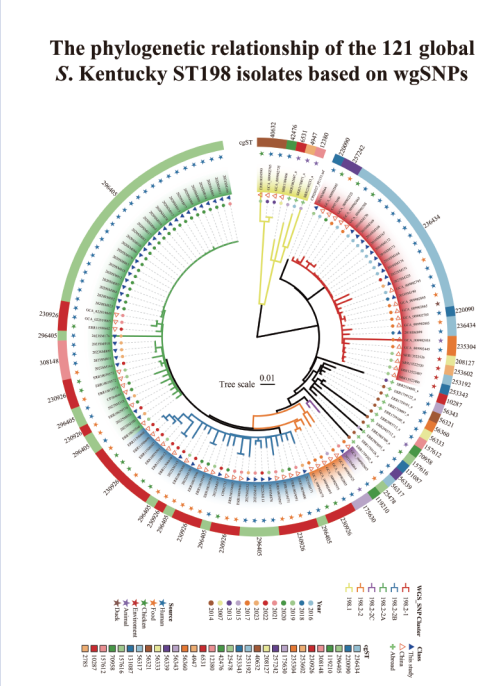

The phylogenetic relationship of the 121 global *S.* Kentucky ST198 isolates based on wgSNPs

ISSN 2096-7071

China CDC Weekly

Editorial Board

Editor-in-Chief Hongbing Shen

Founding Editor George F. Gao

Deputy Editor-in-Chief Liming Li Gabriel M Leung Zijian Feng

Executive Editor Chihong Zhao

Members of the Editorial Board

Rui Chen	Wen Chen	Xi Chen (USA)	Zhuo Chen (USA)
Gangqiang Ding	Xiaoping Dong	Pei Gao	Mengjie Han
Yuantao Hao	Na He	Yuping He	Guoqing Hu
Zhibin Hu	Yueqin Huang	Na Jia	Weihua Jia
Zhongwei Jia	Guangfu Jin	Xi Jin	Biao Kan
Haidong Kan	Ni Li	Qun Li	Ying Li
Zhenjun Li	Min Liu	Qiyong Liu	Xiangfeng Lu
Jun Lyu	Huilai Ma	Jiaqi Ma	Chen Mao
Xiaoping Miao	Ron Moolenaar (USA)	Daxin Ni	An Pan
Lance Rodewald (USA)	William W. Schluter (USA)	Yiming Shao	Xiaoming Shi
Yuelong Shu	RJ Simonds (USA)	Xuemei Su	Chengye Sun
Quanfu Sun	Xin Sun	Feng Tan	Jinling Tang
Huaqing Wang	Hui Wang	Linhong Wang	Tong Wang
Guizhen Wu	Jing Wu	Xifeng Wu (USA)	Yongning Wu
Min Xia	Ningshao Xia	Yankai Xia	Lin Xiao
Wenbo Xu	Hongyan Yao	Zundong Yin	Dianke Yu
Hongjie Yu	Shicheng Yu	Ben Zhang	Jun Zhang
Liubo Zhang	Wenhua Zhao	Yanlin Zhao	Xiaoying Zheng
Maigeng Zhou	Xiaonong Zhou	Guihua Zhuang	

Advisory Board

Director of the Advisory Board Jiang Lu

Vice-Director of the Advisory Board Yu Wang Jianjun Liu Jun Yan

Members of the Advisory Board

Chen Fu	Gauden Galea (Malta)	Dongfeng Gu	Qing Gu
Yan Guo	Ailan Li	Jiafa Liu	Peilong Liu
Yuanli Liu	Kai Lu	Roberta Ness (USA)	Guang Ning
Minghui Ren	Chen Wang	Hua Wang	Kean Wang
Xiaoqi Wang	Zijun Wang	Fan Wu	Xianping Wu
Jingjing Xi	Jianguo Xu	Gonghuan Yang	Tilahun Yilma (USA)
Guang Zeng	Xiaopeng Zeng	Yonghui Zhang	Bin Zou

Editorial Office

Directing Editor Chihong Zhao

Managing Editors Yu Chen

Senior Scientific Editors Daxin Ni Ning Wang Wenwu Yin Shicheng Yu Jianzhong Zhang Qian Zhu

Scientific Editors

Weihong Chen	Tao Jiang	Xudong Li	Nankun Liu	Liwei Shi	Liuying Tang
Meng Wang	Zhihui Wang	Qi Yang	Qing Yue	Lijie Zhang	Ying Zhang

Cover Image: adapted from the article titled "Prevalence and Genomic Characterization of Multidrug-Resistant *Salmonella enterica* Serovar Kentucky Sequence Type 198 Circulating — Beijing Municipality, China, 2016–2023".

Vital Surveillances

Prevalence and Genomic Characterization of Multidrug-Resistant *Salmonella enterica* Serovar Kentucky Sequence Type 198 Circulating — Beijing Municipality, China, 2016–2023

Mei Qu[1]; Ying Huang[1]; Bing Lyu[1]; Xin Zhang[1]; Yi Tian[1]; Zhaomin Feng[1]; Zhiyong Gao[1]; Daitao Zhang[1,#]

ABSTRACT

Introduction: Highly fluoroquinolone-resistant *Salmonella enterica* serovar Kentucky (*S.* Kentucky) of sequence type (ST) 198 has emerged as a global multidrug-resistant (MDR) clone, posing a threat to public health.

Methods: Whole genome sequencing and antibiotic susceptibility testing was used to characterize the population structure and evolutionary history of 54 *S.* Kentucky isolates recovered from food and human clinical cases in Beijing from 2016 to 2023.

Results: All 54 *S.* Kentucky ST198 isolates exhibited resistance to quinolones, carrying point mutations in the quinolone resistance-determining regions (*gyrA*_S83F and *parC*_S80I). Resistance to other antibiotics (folate pathway inhibitors, cephems, aminoglycosides, phenicols, rifamycin, fosfomycin, macrolides, and tetracyclines), mediated by the *sul1*, *sul2*, *dfrA14*, $bla_{\text{CTX-M}}$, $bla_{\text{TEM-1B}}$, *aac(3)-Id*, *aadA2*, *aadA7*, *aph(3')-I*, *aph(3'')-Ib*, *rmtB*, *floR*, *arr-2*, *fosA*, *mph(A)*, and *tet(A)* genes, was also observed in different combinations. The Beijing *S.* Kentucky ST198 evolutionary tree was divided into clades 198.2-1 and 198.2-2, which were further differentiated into three subclades: 198.2-2A, 198.2-2B, and 198.2-2C. Compared with the extended-spectrum β-lactamase-encoding gene $bla_{\text{CTX-M-14b}}$ in 198.2-1, the co-existence of $bla_{\text{CTX-M-55}}$ and $bla_{\text{TEM-1B}}$, as well as chromosomally located *qnrS1*, was detected in most 198.2-2 isolates, which showed more complex MDR phenotypes. *S.* Kentucky ST198 outbreak isolates derived from two predominant clonal sources: 198.2-1 with cgST236434 and 198.2-2A with cgST296405.

Conclusions: The *S.* Kentucky population in Beijing is genetically diverse, consisting of multiple co-circulating lineages that have persisted since 2016. Strengthening surveillance of food and humans will aid in implementing measures to prevent and control the spread of AMR.

Nontyphoidal *Salmonella enterica* infections, particularly those caused by antimicrobial-resistant strains, are a major public health concern (*1*). Notably, fluoroquinolone (FQ)-resistant *Salmonella* spp. and extended-spectrum β-lactamase (ESBL)-producing Enterobacteriaceae were listed by the World Health Organization in 2017 as high-priority pathogens posing the greatest threat to human health (*2*).

Resistance to these antimicrobials has been observed in *S. enterica* serotype Kentucky since the 2000s (*3*–*5*). Highly FQ-resistant *S.* Kentucky has become widespread in recent years (*6*), largely associated with the spread of ST198, which is the most common ST leading to human infections worldwide. Recently, a high prevalence of *S.* Kentucky ST198 with resistance to CIP and extended-spectrum cephalosporins (ESCs) was detected in human, environmental, and chicken samples in China (*7*–*8*).

In this study, we generated a genomic collection of 54 *S.* Kentucky ST198 strains recovered from an active surveillance system in Beijing over an 8-year period from 2016 to 2023. Our aim was to characterize the genetic features and antimicrobial resistance (AMR) profiles of *S.* Kentucky ST198 in Beijing.

METHODS

Sample Collection and Salmonella Identification

Hospital-based active surveillance was conducted from 2010 onward in Beijing, China. From January 2016 to December 2023, a total of 41,742 diarrheal samples were collected from outpatients with gastroenteritis. Various food samples of animal origin were collected from retail outlets and supermarkets to screen for *Salmonella* spp. for food safety risk surveillance. All specimens were processed by routine

microbiologic and biochemical tests to identify *Salmonella*. The *Salmonella* Kentucky serotype was detected by a slide agglutination test using commercially available antisera (SSI Diagnostica, Denmark) according to the White-Kauffmann-Le Minor scheme.

Antimicrobial Susceptibility Testing

Antimicrobial susceptibility testing of *Salmonella* strains was conducted using the broth microdilution method following the guidelines of the Clinical and Laboratory Standards Institute document (CLSI M100-S29:2019). Twenty-eight antimicrobial agents belonging to 12 categories were tested: ampicillin (AMP), ampicillin-sulbactam (AMS), amoxicillin-clavulanic acid (AMC), cefazolin (CFZ), cefoxitin (CFX), cefotaxime (CTX), ceftazidime (CAZ), cefepime (FEP), kanamycin (KAN), gentamicin (GEN), streptomycin (STR), amikacin (AMI), tetracycline (TET), doxycycline (DOX), minocycline (MIN), nalidixic acid (NAL), ciprofloxacin (CIP), levofloxacin (LEV), gemifloxacin (GMI), sulfisoxazole (Sul), trimethoprim-sulfamethoxazole (SXT), chloramphenicol (CHL), azithromycin (AZI), aztreonam (AZM), colistin (CT), polymyxin B (PB), imipenem (IMP) and meropenem (MEM). An MDR phenotype was defined as resistant to at least three classes of antibiotics.

Whole-Genome Sequencing (WGS) and Genomic Analysis

DNA was extracted using a QIAamp DNA Mini Kit (Qiagen, Hilden, Germany). Genomic DNA concentration was determined by agarose gel electrophoresis and fluorometric analysis (Qubit 2.0). WGS was conducted using an Illumina PE150 platform with 100× coverage (Novogene Technology Co., Ltd, Beijing, China). Raw sequencing data were quality-checked, trimmed, and assembled *de novo* into a draft genome sequence using SPAdes 3.13.

Core genome multi-locus sequence typing (cgMLST) was performed using the BacWGSTdb service. AMR genes were screened using the NCBI AMRFinderPlus tool 3.1.1b (https://ftp.ncbi.nlm.nih.gov/pathogen/Antimicrobial_resistance/AMRFinder/). Whole genome single nucleotide polymorphism (wgSNP) analysis for all draft genomes was conducted using snippy pipeline v.4.4.5 with the reference strain *S.* Kentucky ST198 PU131 (GenBank ID: CP026327). Single nucleotide polymorphism (SNP) distance matrices were obtained for all isolates using snp-dist v.0.6.3. The phylogenetic tree and heatmap of resistance genes were visualized using ChiPlot (https://www.chiplot.online/).

Results

Epidemiological Information for *S.* Kentucky ST198 Isolates from Beijing

Between 2016 and 2023, an active surveillance system collected 1,838 *S. enterica* strains, of which 54 (2.9%) were *S.* Kentucky isolates. All 54 *S.* Kentucky isolates were assigned to ST198. Forty-nine were collected from patients with clinical diarrhea, and five were isolated from chicken meat. Eight and 23 of the 54 strains were from two outbreaks in 2016 and 2020, respectively, while the remaining isolates were from sporadic cases. These 54 strains were isolated between 2016 and 2023, with the following annual distribution: eight in 2016, two in 2018, two in 2019, 23 in 2020, three in 2021, seven in 2022, and nine in 2023. The strains were distributed across 12 districts.

Antibiotic Resistance and MDR Profiles

All 54 *S.* Kentucky isolates were resistant to quinolones (NAL, CIP, LEV, and GMI), tetracyclines (TET and DOX), folate pathway inhibitors (Sul), and susceptible to carbapenems (IMP and MEM). Regarding cephems, *S.* Kentucky isolates showed the highest resistance to CFZ (90.7%), followed by CTX (87.0%), FEP (85.2%), and CAZ (63.0%). However, resistance to AMC, FOX, CT, and PB was relatively low, at only 1.9%. The frequency of AMR is presented in Figure 1. In addition, 85.2% (46/54) of ST198 isolates were ESBL-producing strains.

All 54 isolates (100%) were resistant to at least four antimicrobial classes. Resistance to six, eight, and 10 classes was observed in 94.4%, 83.3%, and 53.7% of isolates, respectively.

Phylogenetic Analysis of Global *S.* Kentucky ST198 Isolates

To reveal the genetic relatedness of *S.* Kentucky ST198 isolates, a global phylogenetic tree was constructed using 121 isolates, including 15 global strains, 52 Chinese isolates obtained from 11 other Provincial-level administrative divisions (PLADs), and the 54 isolates from this study (Figure 2). As previously reported (*9*), the *S.* Kentucky ST198 isolates were

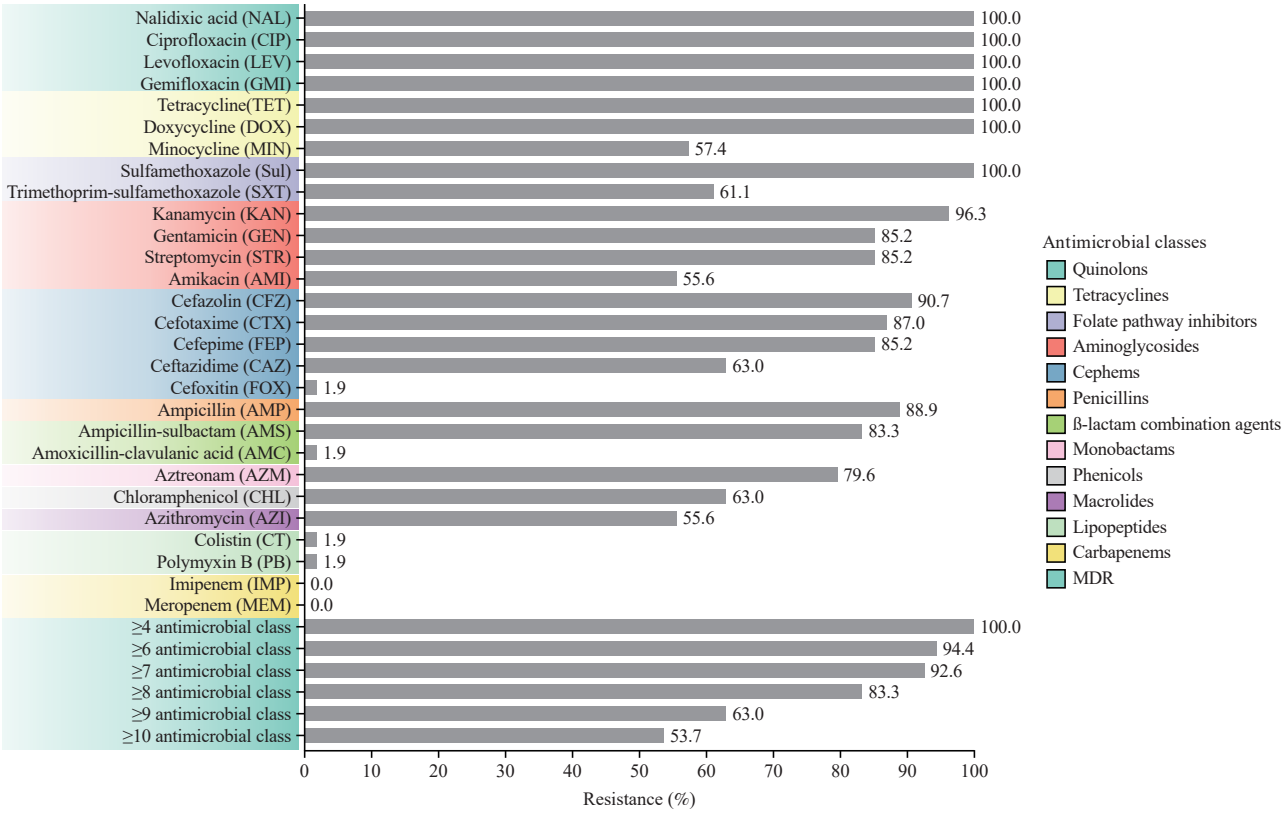

FIGURE 1. Antimicrobial resistance of 54 *S.* Kentucky isolates against 28 antimicrobial agents belonging to 12 categories.
Abbreviation: *S.* Kentucky=*Salmonella* Kentucky; MDR=multidrug resistant.

divided into two clades, 198.1 and 198.2. Clade 198.2 was further subdivided into two subclades, 198.2-1 and 198.2-2. The 15 global strains were mainly distributed in clades 198.1, 198.2-1, and 198.2-2. Although the Chinese isolates showed significant diversity, they were concentrated in clades 198.1 (3.3%, 4/121), 198.2-1 (24.0%, 29/121), and 198.2-2 (60.3%, 73/121). Furthermore, 30 subclade 198.2-1 isolates obtained from five provincial-level administrative divisions (PLADs), including Xichuan, Guangxi, Hunan, Jiangsu, and Zhejiang, were detected between 2013 and 2023, while 73 subclade 198.2-2 isolates obtained from nine PLADs (Anhui, Fujian, Guangdong, Guangxi, Guizhou, Jiangsu, Liaoning, Shandong, and Zhejiang) were collected from 2015 to 2022. Strains from various sources (animal, chicken, duck, environment, food, and human) clustered together, implying cross-transmission between hosts.

To reveal the molecular characteristics of *S.* Kentucky ST198 isolates, we performed cgMLST on the whole-genome sequences of the 121 global isolates and identified 31 cgSTs (Figure 2). The most common cgSTs were cgST296405 (30.6%), followed by cgST230926 (23.1%) and cgST236434 (15.7%). Twenty-two cgSTs were represented by only one isolate, and cgST40632 was detected only in three clade 198.1 isolates. Among the 30 subclade 198.2-1 isolates, nine cgSTs were detected, with cgST236434 being the predominant type, accounting for 63.3% (19/30). By contrast, only six cgSTs were identified in 73 subclade 198.2-2 isolates, with cgST296405 accounting for 50.7% (37/73) and cgST230926 accounting for 38.4% (28/73).

Diversity and Discrepancy of *S.* Kentucky ST198 Isolates from Beijing

Phylogenetic analysis of the 54 Beijing isolates was performed (Figure 3A), and a heatmap of SNPs was generated (Figure 3B). The number of SNPs ranged from 15 to 100 between food-derived isolates, from 0 to 103 between human-derived isolates, and from 9 to 102 between human- and food-derived isolates. Of the 54 Beijing isolates, 13 (24.1%), 32 (59.3%), 8 (14.8%), and 1 (1.9%) belonged to subclades 198.2-1, 198.2-2A, 198.2-2B, and 198.2-2C, respectively (Figure 3A). Thirteen isolates were distributed in subclade 198.2-1: one clustered with eight strains from outbreak 1 in 2016 (0 SNPs) in one branch, and the

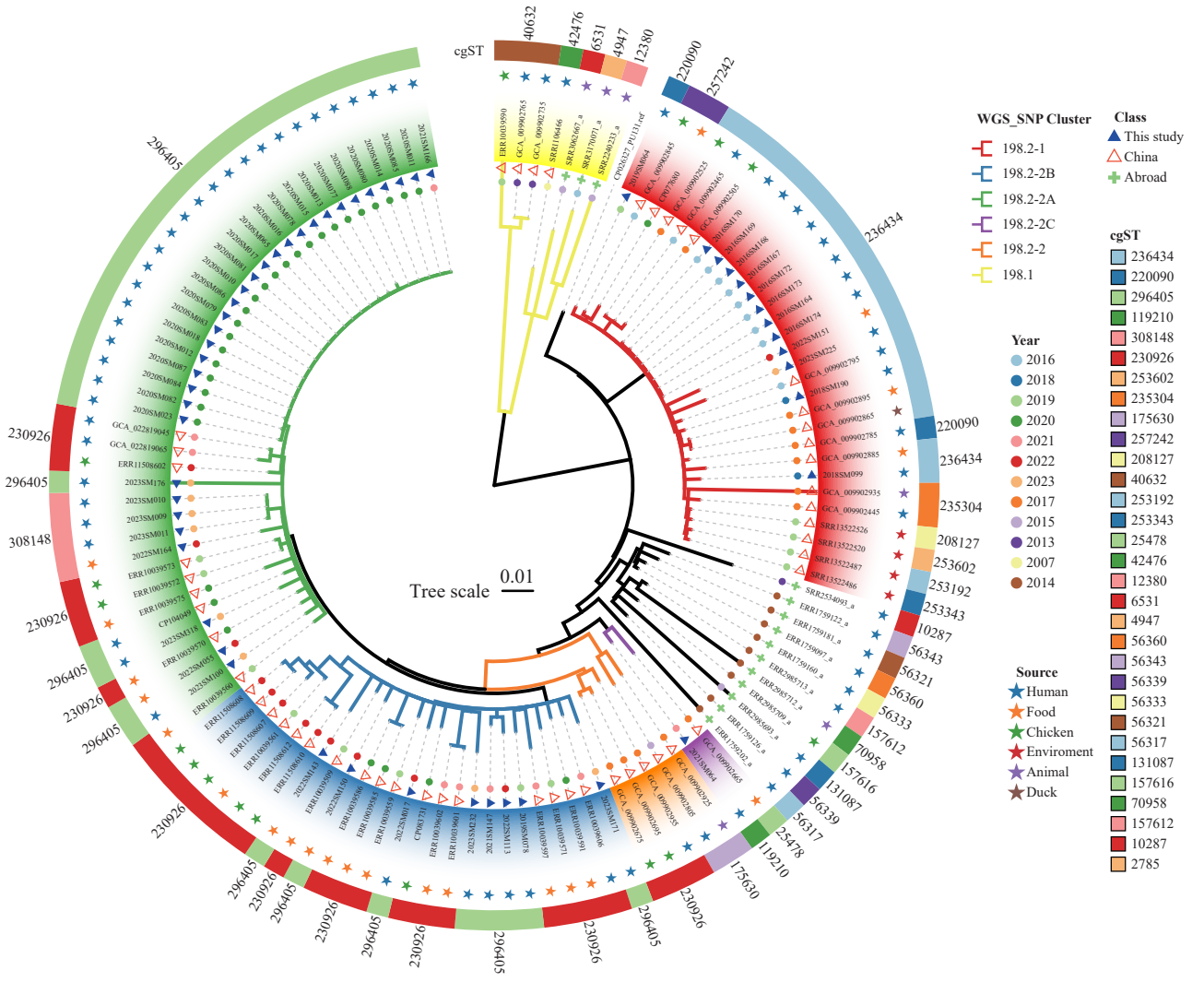

FIGURE 2. The phylogenetic relationship of the 121 global *S.* Kentucky ST198 isolates based on wgSNPs.
Note: In the two outer circles, the cgSTs are shown in colored rings, and the sources of strains are shown in colored pentagrams. In the two inner circles, the isolation year of strains is indicated by colored dots, and strains from this study are shown as filled blue triangles, strains from China are shown as hollow red triangles, and global strains are shown as filled green crosses. The tree branches are color-coded to highlight *S.* Kentucky strains from clades 198.1, 198.2-1, 198.2-2, and sub-cluster 198.2-2 (2A-2C).
Abbreviation: *S.* Kentucky=*Salmonella* Kentucky; ST=sequence type; wgSNPs=whole genomic single nucleotide polymorphisms; cgST=core genomic sequence type.

other clustered with five sporadic strains from 2018 and 2019 (1–4 SNPs). In subclade 198.2-2A, 23 strains from outbreak 2 in 2020 clustered together (0–1 SNP), along with nine sporadic strains, including seven human isolates from 2021 and 2023, and two food isolates (chicken meat) from 2022 (1–5 SNPs). In subclade 198.2-2B, the majority of isolates (n=8) clustered with six strains from humans (2019–2023) and two strains from food (2022) (1–4 SNPs). The remaining human isolate (2021SM064) in subclade 198.2-2C was distantly related to other Beijing isolates (22–31 SNPs).

The 54 Beijing isolates yielded five cgSTs: cgST296405 (66.7%), cgST236434 (22.2%), cgST308148 (7.4%), cgST220090 (1.9%), and cgST119210 (1.9%). The cgST296405 genotype was most prevalent, comprising 23 outbreak strains from 2020 and 13 sporadic strains from 2019 (n=1), 2021 (n=2), 2022 (n=5), and 2023 (n=5). The cgST236434 genotype included eight outbreak isolates from 2016 and four sporadic isolates from 2018 (n=2), 2022 (n=1), and 2023 (n=1). These findings were consistent with SNP analysis, suggesting that cgST296405 and cgST236434 represent two major endemic genotypes in Beijing.

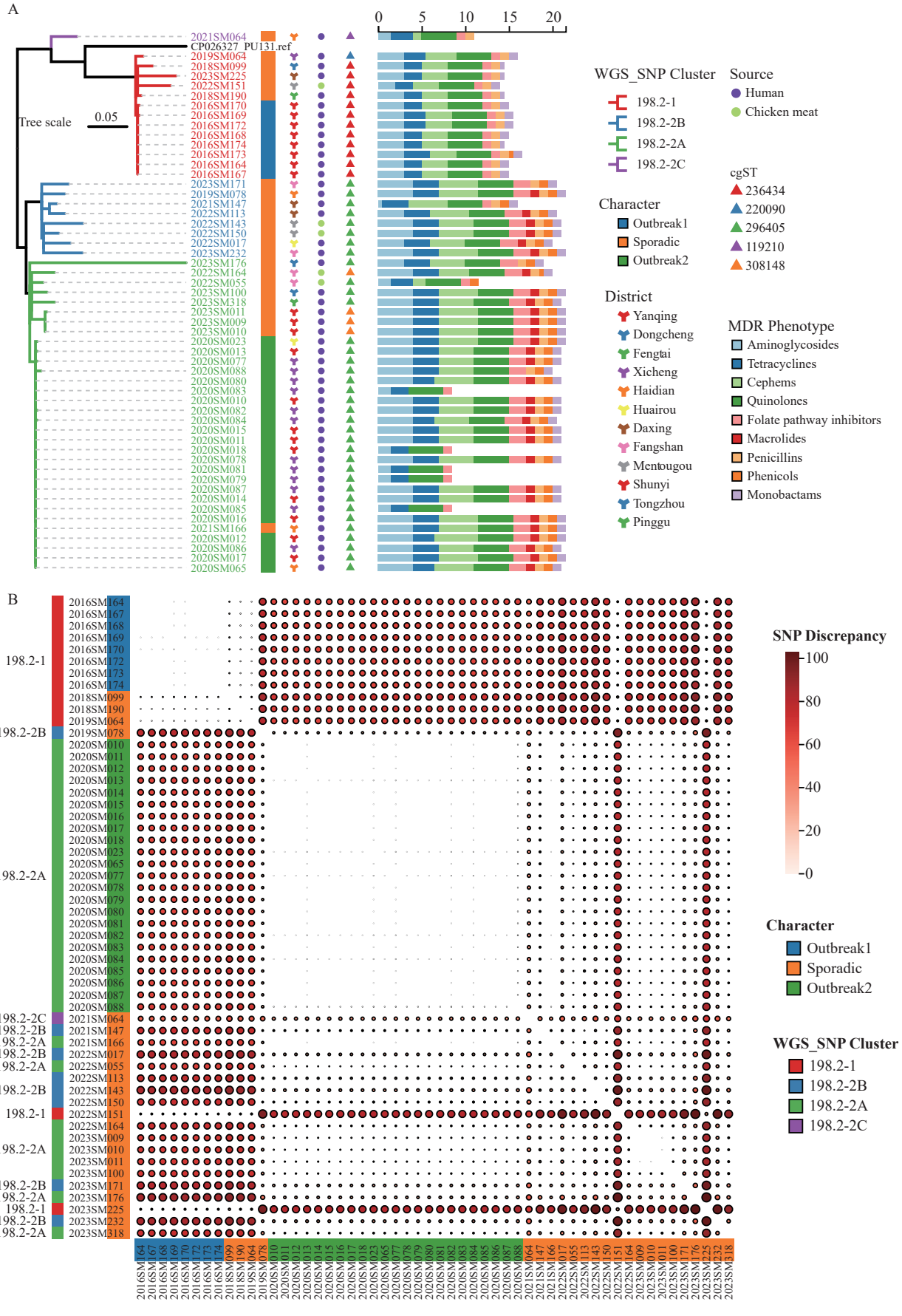
A
0
5
10
15
20
Tree scale
0.05
CP026327_PU131.ref
WGS_SNP Cluster
198.2-1
198.2-2B
198.2-2A
198.2-2C
Source
Human
Chicken meat
cgST
236434
220090
296405
119210
308148
Character
Outbreak1
Sporadic
Outbreak2
District
Yanqing
Dongcheng
Fengtai
Xicheng
Haidian
Huairou
Daxing
Fangshan
Mentougou
Shunyi
Tongzhou
Pinggu
MDR Phenotype
Aminoglycosides
Tetracyclines
Cephems
Quinolones
Folate pathway inhibitors
Macrolides
Penicillins
Phenicols
Monobactams
B
198.2-1
198.2-2B
198.2-2A
198.2-2C
SNP Discrepancy
100
80
60
40
20
0
Character
Outbreak1
Sporadic
Outbreak2
WGS_SNP Cluster
198.2-1
198.2-2B
198.2-2A
198.2-2C

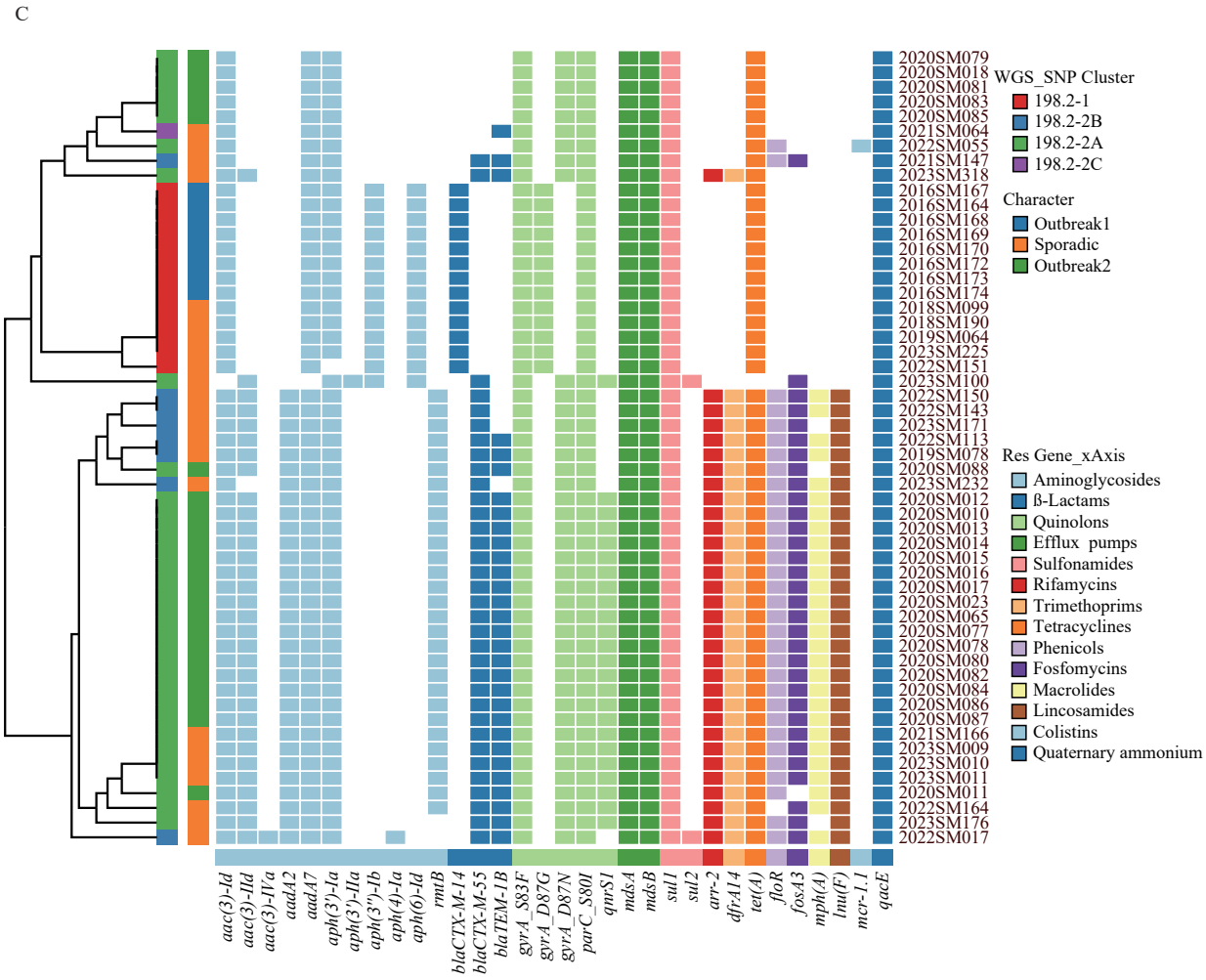

FIGURE 3. Phylogenetic analysis and the AMR phenotypic and genotypic characteristics of the 54 *S.* Kentucky isolates from Beijing. (A) The phylogenetic relationships, epidemiological and molecular features, and the MDR phenotypes of the 54 *S.* Kentucky isolates. (B) The matrix of SNPs for the 54 *S.* Kentucky isolates shows all correlations between outbreak and sporadic strains, as well as the various sources. (C) A heatmap of AMR genes. The color blocks on the X-axis represent the categories of genes. Colored cells represent the presence of genes, and white cells represent the absence of genes.
Note: The size of the circle represents the number of SNP differences between two isolates: the larger the circle, the greater the number of SNP differences, and no circle indicates no difference (0 SNPs).
Abbreviation: AMR=antimicrobial resistance; *S.* Kentucky=*Salmonella* Kentucky; MDR=multidrug resistant; SNP=single nucleotide polymorphism.

Resistomes of *S.* Kentucky ST198 Isolates from Beijing

To characterize the AMR profiles of the *S.* Kentucky ST198 isolates from Beijing, we scanned the genomes to identify AMR-related genes and mutations. We detected 32 AMR genes in 14 classes, including those involved in resistance to aminoglycosides (11 genes), β-lactams (3 genes), quinolones (1 gene and 4 point mutations), efflux pumps (2 genes), sulfonamides (2 genes), rifamycins (1 gene), trimethoprims (1 gene), tetracycline (1 gene), phenicols (1 gene), fosfomycin (1 gene), macrolides (1 gene), lincosamides (1 gene), colistins (1 gene), and quaternary ammonium (1 gene) (Figure 3C). Resistance genes from seven classes were found in strains within clade 198.2-1, while 14 classes were found in strains within clade 198.2-2.

The AMR gene profiles and phenotypes differed between the subclade 198.2-1 and 198.2-2 strains (Figure 3A and 3C). For β-lactamase resistance genes, $bla_{\text{CTX-M-14b}}$ was the only gene detected among the 13 subclade 198.2-1 isolates. However, in subclade 198.2-2, $bla_{\text{CTX-M-55}}$ and $bla_{\text{TEM-1B}}$ were detected in 82.9% (34/41) and 73.2% (30/41) of isolates, respectively. For the aminoglycoside resistance gene profiles, *aac(3)-Id*, *aadA7*, and *aph(3')-Ia* genes were

detected in 98.1% (53/54) of isolates, and the *aph(3'')-Ib* gene was detected in 25.9% (14/54) of isolates. The *aac(3)-IId*, *aadA2*, and *rmtB* genes were only detected in subclade 198.2-2, accounting for 78.0% (32/41), 75.6% (31/41), and 70.7% (29/41) of isolates, respectively. The *aph(3'')-Ib* and *aph(6)-Id* genes were detected in all 41 subclade 198.2-1 isolates but only one subclade 198.2-2 isolate. For tetracycline resistance genes, *tet(A)* was detected in all 198.2-1 isolates and 97.6% (40/41) of 198.2-2 isolates. For folate pathway antagonist genes, *sul1* was prevalent in all isolates, and *sul2* was only detected in two 198.2-2 isolates. The *dfrA14* and *floR* genes were detected in 78.0% (32/41) of the 198.2-2 isolates. Additionally, all strains resistant to SXT carried at least one gene associated with resistance to folate pathway antagonists. The genes *lnu(F)*, *mph(A)*, *arr-2*, and *fosA3*, conferring correspondent resistance to lincosamide, macrolide, rifamycin, and fosfomycin, were only detected in 198.2-2, accounting for 75.6% (31/41), 68.3% (28/41), 78.0% (32/41), and 78.0% of isolates, respectively. For quinolone resistance, the same mutations in *parC*_S80I and *gyrA*_S83F were detected in all 198.2 isolates, but *gyrA*_D87G was present in 198.2-1 isolates, whereas *gyrA*_D87N was present in 198.2-2 isolates. The *qnrS1* gene was only detected in 58.5% (24/41) of 198.2-2 isolates. Notably, the *mcr-1* gene was detected in only one strain, 2022SM055 from chicken meat, which was found to be resistant to colistin. Importantly, the 198.2-2 isolates showed more complex AMR phenotypes and carried more resistance genes than the 198.2-1 isolates.

Spatiotemporal Distribution and Phylogenetic Relationship of Sporadic and Outbreak *S.* Kentucky Strains in Beijing

To demonstrate the evolutionary relationships of *S.* Kentucky strains from different sources in Beijing, a Sankey diagram was constructed (Figure 4). The first outbreak, occurring in Yanqing District in 2016,

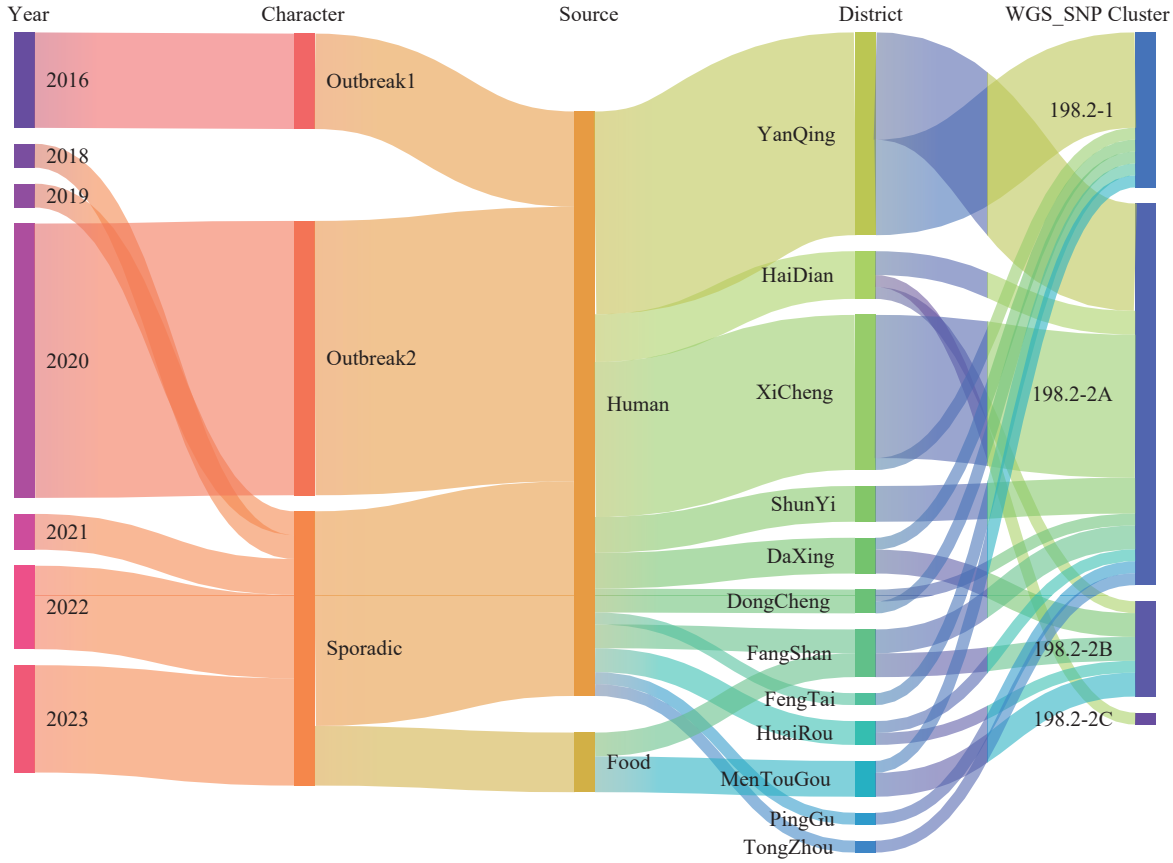

FIGURE 4. A Sankey diagram demonstrating the spatiotemporal distribution and the transmission of multiple lineages of *S.* Kentucky strains in Beijing.
Abbreviation: *S.* Kentucky=*Salmonella* Kentucky.

involved eight human-derived strains belonging to phylogenetic lineage 198.2-1 and cgST236434 (Figure 2, Figure 4). The second outbreak, occurring in four districts (Xicheng, Yanqing, Haidian, and Huairou) in 2020, involved 23 human-derived strains grouped in lineage 198.2-2A and cgST296405, suggesting cross-regional transmission and clonal expansion during this outbreak. The remaining 23 sporadic cases, distributed across 11 districts (Daxing, Docheng, Fangshan, Fengtai, Haidian, Huairou, Mentougou, Pinggu, Shunyi, Tongzhou, and Xicheng) between 2018 and 2023, included 18 human-derived and five chicken meat-derived strains. These sporadic strains derived from a polyclonal evolutionary source (198.2-1, 198.2-2A, 198.2-2B, and 198.2-2C) and formed five cgMLST groups. The five chicken meat isolates, distributed across two districts in 2022, were mainly from lineages 198.2-1, 198.2-2A, and 198.2-2B and were closely related to human isolates. These results suggest that the *S.* Kentucky ST198 outbreak isolates have two predominant clonal sources: 198.2-1 with cgST236434 before 2019 and 198.2-2A with cgST296405 after 2019.

DISCUSSION

S. Kentucky ST198 has been increasingly reported in chickens and can cause human infections in China (*8*–*9*). In this study, all 54 *S.* Kentucky isolates were assigned to ST198. Our findings showed that the positive ratio for *S.* Kentucky ST198 among *S.* enterica isolates was 2.9% (54/1,838) in Beijing, which is approximately fourfold higher than that reported in a previous study (0.39%, 40/16,247) (*9*) and much higher than that reported in Shenzhen (0.7%, 57/8,559) (*10*) and among patients (0.33%, 40/12,011) in China between 2010 and 2016 (*8*).

In the present study, genomic analyses (cgMLST and wgSNP) were conducted to characterize the *S.* Kentucky ST198 strains. Five cgSTs were identified, with cgST296405 and cgST236434 being the predominant genotypes causing outbreaks. Phylogenetic analysis indicated that the 54 *S.* Kentucky strains clustered into lineages 198.2-1 and 198.2-2, then further divided into three sublineages, 198.2-2A, 198.2-2B, and 198.2-2C, revealing the existence of multiple lineages circulating in Beijing. Additionally, many sublineages were shared by strains from this study and strains from other PLADs, such as Guangxi, Shandong, Fujian, and Zhejiang, indicating a potential phylogenetic relationship between these strains.

In view of the increasing public health threat posed by the global emergence and dissemination of antimicrobial-resistant *S.* Kentucky, this investigation revealed a high level of both phenotypic and genotypic resistance to different classes of antimicrobials among 54 *S.* Kentucky isolates. The isolates were resistant to ESCs as follows: CTX (87.0%, 47/54), CAZ (63.0%, 34/54), and FEP (85.2%, 46/54). Resistance to ESCs is normally mediated by the production of ESBLs, and CTX-M-type ESBLs pose a particularly serious public health threat worldwide (*11*). In this study, all Beijing isolates in subclade 198.2-1 carried the gene $bla_{\text{CTX-M-14b}}$, consistent with previous studies in China (*6*–*7*,*9*,*12*), indicating the formation of a clade carrying $bla_{\text{CTX-M-14b}}$ in China. In addition, compared with $bla_{\text{CTX-M-14b}}$ in 198.2-1, the co-existence of $bla_{\text{CTX-M-55}}$ and $bla_{\text{TEM-1B}}$ was detected in the majority of 198.2-2 isolates. It is worth mentioning that all *S.* Kentucky isolates in this study were resistant not only to CIP but also to other FQ antibiotics (LEV, GMI), showing substantially higher levels of resistance than previously reported for *S.* Kentucky in China or many other countries (*6*,*8*,*13*). Moreover, all strains carried two quinolone resistance-determining region mutations (*gyrA*_S83F and *parC*_S80I), but *qnrS1* and *gyrA*_D87N were only detected in 198.2-2 isolates. Several studies reported the presence of the *qnrS1* gene on the bacterial chromosome, along with a large number of chromosomally-located resistance genes, after 2017. The emergence of *qnrS1* in *S.* Kentucky isolates with *gyrA* and *parC* mutations increased bacterial resistance to CIP (*10*,*12*). In the present study, up to 85.2% of isolates were both FQ-resistant and ESBL-producing, confirming these as common features of *S.* Kentucky. Our study further revealed that the acquisition of an MDR phenotype by 198.2-2 has potentially contributed to its higher prevalence compared with 198.2-1, making it the most prevalent subclade for clonal transmission in Beijing.

In conclusion, the human salmonellosis epidemic caused by *S.* Kentucky involved multiple native circulating lineages that have become widely distributed across Beijing districts since 2016. Many clinical isolates were genetically clonal to strains isolated from food, suggesting possible cross-host transmission. Increased genome sequencing of strains from various host sources will facilitate the identification of transmission routes and determine potential ongoing outbreaks, which is vital for formulating targeted surveillance and countermeasures.

Conflicts of interest: No conflicts of interest.

doi: 10.46234/ccdcw2024.179

[#] Corresponding author: Daitao Zhang, zdt016@163.com.

[1] Beijing Key Laboratory of Diagnostic and Traceability Technologies for Food Poisoning, Beijing Center for Disease Prevention and Control, Beijing, China.

Submitted: April 26, 2024; Accepted: August 03, 2024

REFERENCES

1. Majowicz SE, Musto J, Scallan E, Angulo FJ, Kirk M, O'Brien SJ, et al. The global burden of nontyphoidal *Salmonella* gastroenteritis. Clin Infect Dis 2010;50(6):882 – 9. https://doi.org/10.1086/650733.
2. Tacconelli E, Carrara E, Savoldi A, Harbarth S, Mendelson M, Monnet DL, et al. Discovery, research, and development of new antibiotics: the WHO priority list of antibiotic-resistant bacteria and tuberculosis. Lancet Infect Dis 2018;18(3):318 – 27. https://doi.org/10.1016/S1473-3099(17)30753-3.
3. Le Hello S, Hendriksen RS, Doublet B, Fisher I, Nielsen EM, Whichard JM, et al. International spread of an epidemic population of *Salmonella enterica* serotype Kentucky ST198 resistant to ciprofloxacin. J Infect Dis 2011;204(5):675 – 84. https://doi.org/10.1093/infdis/jir409.
4. Le Hello S, Harrois D, Bouchrif B, Sontag L, Elhani D, Guibert V, et al. Highly drug-resistant *Salmonella enterica* serotype Kentucky ST198-X1: a microbiological study. Lancet Infect Dis 2013;13(8):672 – 9. https://doi.org/10.1016/S1473-3099(13)70124-5.
5. Le Hello S, Bekhit A, Granier SA, Barua H, Beutlich J, Zając M, et al. The global establishment of a highly-fluoroquinolone resistant *Salmonella enterica* serotype Kentucky ST198 strain. Front Microbiol 2013;4:395. https://doi.org/10.3389/fmicb.2013.00395.
6. Hawkey J, Le Hello S, Doublet B, Granier SA, Hendriksen RS, Fricke WF, et al. Global phylogenomics of multidrug-resistant *Salmonella enterica* serotype Kentucky ST198. Microb Genom 2019;5(7):e000269. https://doi.org/10.1099/mgen.0.000269.
7. Chen HH, Song JJ, Zeng XY, Chen DD, Chen RC, Qiu C, et al. National prevalence of *Salmonella enterica* serotype Kentucky ST198 with high-level resistance to ciprofloxacin and extended-spectrum cephalosporins in China, 2013 to 2017. mSystems 2021;6(1):e00935 – 20. https://doi.org/10.1128/mSystems.00935-20.
8. Xiong ZY, Wang SJ, Huang YM, Gao Y, Shen HY, Chen ZQ, et al. Ciprofloxacin-resistant *Salmonella enterica* serovar Kentucky ST198 in broiler chicken supply chain and patients, China, 2010-2016. Microorganisms 2020;8(1):140. https://doi.org/10.3390/microorganisms8010140.
9. Wang J, Jiang Y, Ji RY, Wang ZY, Lu MJ, Wu H, et al. Colistin- and tigecycline-resistant CTX-M-14-producing *Salmonella enterica* serovar Kentucky ST198 from retail chicken meat, China. Int J Antimicrob Agents 2022;59(2):106504. https://doi.org/10.1016/j.ijantimicag.2021.106504.
10. She YY, Jiang YX, Luo MM, Duan XK, Xie L, Yang C, et al. Emergence of chromosomally located $bla_{\text{CTX-M-14b}}$ and *qnrS1* in *Salmonella enterica* serotype Kentucky ST198 in China. Int J Antimicrob Agents 2023;62(3):106896. https://doi.org/10.1016/j.ijantimicag.2023.106896.
11. Ho PL, Lo WU, Yeung MK, Li Z, Chan J, Chow KH, et al. Dissemination of pHK01-like incompatibility group IncFII plasmids encoding CTX-M-14 in *Escherichia coli* from human and animal sources. Vet Microbiol 2012;158(1-2):172 – 9. https://doi.org/10.1016/j.vetmic.2012.02.004.
12. Xu HY, Cao XL, Zhang WB, Li QC. Co-existence of two ciprofloxacin-resistant *Salmonella enterica* serovar Kentucky strains in the urine of a bladder cancer patient. J Glob Antimicrob Resist 2022;30:354 – 6. https://doi.org/10.1016/j.jgar.2022.07.011.
13. Haley BJ, Kim SW, Haendiges J, Keller E, Torpey D, Kim A, et al. *Salmonella enterica* serovar Kentucky recovered from human clinical cases in Maryland, USA (2011-2015). Zoonoses Public Health 2019;66(4):382 – 92. https://doi.org/10.1111/zph.12571.

Vital Surveillances

Post-Marketing Surveillance of Adverse Events Following Immunization with *Haemophilus Influenzae* Type b Conjugate Vaccine — China, 2010–2021

Minrui Ren[1]; Keli Li[1,#]; Yan Li[1]; Chunxiang Fan[1]; Yuyang Xu[1,2]; Lina Zhang[1]; Yuan Li[1]; Lei Cao[1]; Wenzhou Yu[1]; Zundong Yin[1]

ABSTRACT

Introduction: The *Haemophilus influenzae* type b (Hib) conjugate vaccine is widely administered in China.

Methods: We extracted data on Hib vaccine doses administered and adverse events following immunization (AEFI) reported between 2010 and 2021 from the Chinese National Immunization Information System (CNIIS). A descriptive analysis was conducted to examine the characteristics and incidence rates of AEFI with the Hib vaccine.

Results: In China, between 2010 and 2021, a total of 52,910 AEFIs with the Hib vaccine were reported, resulting in an overall AEFI reporting rate of 38.10 per 100,000 doses. Common (typically minor) and rare (potentially serious) vaccine reactions occurred at rates of 34.71 and 2.78 per 100,000 doses, respectively. Among the common vaccine reactions, the incidences of fever (axillary temperature ≥38.6 ℃), injection site redness and swelling (>2.5 cm in diameter), and injection site induration (>2.5 cm in diameter) were 11.93, 9.69, and 3.38 per 100,000 doses, respectively. Rare vaccine reactions included anaphylactic rash, angioedema, and febrile convulsion with reported incidences of 2.42, 0.10, and 0.05 per 100,000 doses, respectively. The incidence of serious rare vaccine reactions was 0.16 per 100,000 doses.

Conclusions: The reported incidence of AEFI with the Hib vaccine was low, with the occurrence of serious rare adverse reactions also being markedly low throughout the period 2010–2021 in China.

Haemophilus influenzae type b (Hib) is a major pathogen responsible for serious illnesses in young children, including pneumonia, meningitis, septicemia, suppurative arthritis, and other invasive infections. The World Health Organization (WHO) estimated that in 2008, approximately 203,000 children under the age of five succumbed to invasive Hib diseases globally (*1*). The Hib conjugate vaccine (Hib vaccine) has proven to be highly effective in preventing these diseases. In China, the Hib vaccine is one of the most broadly utilized vaccines in the non-National Immunization Program (non-NIP). This study analyzed surveillance data on adverse events following immunization (AEFI) with the Hib vaccine, as reported to the Chinese National Immunization Information System (CNIIS) from 2010 to 2021. Notably, this analysis does not include data from Hong Kong SAR, Macau SAR, and Taiwan, China. The findings offer substantial evidence supporting further post-marketing safety assessments of the Hib vaccine.

METHODS

AEFI cases with the Hib vaccine, reported between 2010 and 2021, were sourced from the CNIIS AEFI surveillance module. Data on the number of Hib vaccine doses administered during the study period were obtained from the CNIIS vaccination surveillance module.

Hib vaccines, authorized by various marketing authorization holders (MAHs), are approved for administration in children aged 2 months to 5 years. The standard immunization schedule includes three primary-series doses, administered monthly beginning at 2–3 months, followed by a booster dose at 18 months. Infants initiating Hib vaccination between 6–12 months receive two doses, while children who begin their vaccination between 1–5 years receive a single dose.

AEFI surveillance is conducted in compliance with applicable laws, regulations, and guidelines (*2–3*). Various entities, including medical institutions, vaccination providers, MAHs, CDCs, and medical

associations, have distinct roles in the reporting, investigation, and causality assessment of AEFIs. AEFIs are categorized into reactions related to vaccine products, reactions due to vaccine quality defects, reactions suspected to be caused by immunization errors, coincidental events, and psychogenic reactions. Among these, vaccine product-related reactions, or vaccine reactions, are adverse events that are either confirmed to be caused by the vaccine or cannot be definitively ruled out as being caused by the vaccine. These reactions are further subdivided into common reactions, which are usually minor, and rare reactions, which could be serious. Specific symptoms such as fever (axillary temperature ≥38.6 °C), redness and swelling at the injection site (diameter >2.5 cm), and induration at the injection site (diameter >2.5 cm) are mandated to be reported. Serious AEFI encompasses events that are life-threatening, may result in death, or may lead to substantial or permanent disability or significant impairment of organ function. Serious rare vaccine reactions primarily encompass those serious AEFIs that are suspected to be vaccine-related.

Data were analyzed utilizing Microsoft Office Excel (version 2016, Microsoft, Washington, USA) and R (version 4.2.1, R Foundation for Statistical Computing, Vienna, Austria). Descriptive statistics were employed to elucidate the distributions, characteristics, and reported incidences of AEFI with the Hib vaccine. The incidence of AEFI was calculated by taking the number of reported AEFI cases, multiplying it by 100,000, and then dividing it by the total number of administered doses of the Hib vaccine.

RESULTS

Characteristics of AEFI

From 2010 to 2021, a total of 52,910 AEFIs with the Hib vaccine were reported in China. Of these, 58.01% involved male recipients and 41.99% female recipients, yielding a male-to-female ratio of 1.38∶1. The distribution of AEFI reports by age group showed that 51.01% were in children under 1 year, 36.65% in 1-year-olds, and 12.35% in children aged 2 years or older. Geographically, 60.66% of the reports originated from the eastern regions, 27.53% from the central regions, and 11.81% from the western regions of China. Seasonally, AEFI reports varied across the quarters of the year, comprising 17.38% in the first quarter, 34.33% in the second, 32.70% in the third, and 15.59% in the fourth quarter. The analysis of AEFI reports by dose number revealed that 53.91% occurred after the first dose, 18.15% after the second, 14.97% after the third, and 12.97% after the fourth dose. Additionally, 25.76% of AEFI cases involved children who were concurrently vaccinated with other vaccines. The most commonly co-administered vaccines were the acellular DPT vaccine (7,392 cases, 13.97%), the polio vaccine (2,509 cases, 4.74%), and the meningococcal vaccine (1,407 cases, 2.66%). The timing of AEFI onset post-vaccination was predominantly within the first day (58.42%), followed by 2 to 3 days (39.98%), 4 to 14 days (1.14%), and 15 days or more (0.46%), as summarized in Table 1.

Incidence of AEFI by Year and Cause

Between 2010 and 2021, approximately 138.88 million doses of the Hib vaccine were administered in China. The reported overall rate of AEFIs was 38.10 per 100,000 doses. This rate fluctuated annually, with a low of 18.60 and a high of 50.25 per 100,000 doses. The breakdown of AEFI rates included: common vaccine reactions at 34.71 per 100,000 doses, rare vaccine reactions at 2.78 per 100,000, coincidental events at 0.57 per 100,000, psychogenic reactions at 0.005 per 100,000, suspected immunization error-related reactions at 0.004 per 100,000, and non-classifiable events at 0.02 per 100,000 doses. No event of vaccine quality defect-related reactions was reported. Incidence rates for serious AEFIs were 0.31 per 100,000 doses, for non-serious AEFIs were 37.79 per 100,000 doses, and for serious rare vaccine reactions were 0.16 per 100,000 doses, as detailed in Table 2.

Clinical Diagnoses of Common Vaccine Reactions

The study identified 48,203 cases of common vaccine reactions. Fever (axillary temperature ≥38.6 ℃), injection site redness and swelling (diameter >2.5 cm), and injection site induration (diameter >2.5 cm) represented 34.38%, 27.91%, and 9.74% of these reactions respectively, with incidence rates per 100,000 doses of 11.93, 9.69, and 3.38. Additional reported reactions accounted for 4.67% of the total. The five most commonly observed symptoms among these additional reactions were rash (16.80%), crying (11.38%), vomiting (6.71%), pruritus (4.31%), and diarrhea (3.91%), as detailed in Table 3. The majority of the common vaccine reactions occurred within three days post-vaccination, with proportions of 99.08% for fever, 98.75% for injection site redness and swelling, and 97.93% for injection site induration.

TABLE 1. Characteristics of Hib vaccine AEFI in China, 2010–2021.

Characteristics	AEFI		Serious AEFI		Common vaccine reaction		Rare vaccine reaction	
	Number	Proportion (%)	Number	Proportion (%)	Number	Proportion (%)	Number	Proportion (%)
Sex								
Male	30,693	58.01	252	59.29	27,953	57.99	2,253	58.29
Female	22,217	41.99	173	40.71	20,250	42.01	1,612	41.71
Age group								
<1 years	26,987	51.01	263	61.88	24,346	50.51	2,166	56.04
1–2 years	19,390	36.65	128	30.12	17,697	36.71	1,399	36.20
≥2 years	6,533	12.35	34	8.00	6,160	12.78	300	7.76
Region								
Eastern	32,094	60.66	198	46.59	29,208	60.59	2,415	62.48
Central	14,566	27.53	147	34.59	13,543	28.10	848	21.94
Western	6,250	11.81	80	18.82	5,452	11.31	602	15.58
Quarter								
1	9,195	17.38	112	26.35	8,240	17.09	769	19.90
2	18,166	34.33	105	24.71	16,679	34.60	1,237	32.01
3	17,301	32.70	120	28.24	15,861	32.90	1,200	31.05
4	8,248	15.59	88	20.71	7,423	15.40	659	17.05
Dose number								
1	28,525	53.91	256	60.24	25,831	53.59	2,187	56.58
2	9,601	18.15	80	18.82	8,631	17.91	818	21.16
3	7,919	14.97	49	11.53	7,323	15.19	500	12.94
4	6,865	12.97	40	9.41	6,418	13.31	360	9.31
Vaccinated with other vaccines								
No	39,279	74.24	238	56.00	35,899	74.47	2,803	72.52
Yes	13,631	25.76	187	44.00	12,304	25.53	1,062	27.48
Onset time after vaccination								
0–1 day	30,912	58.42	218	51.29	27,914	57.91	2,504	64.79
2–3 day	21,151	39.98	143	33.65	19,631	40.73	1,235	31.95
4–14 day	604	1.14	47	11.06	478	0.99	81	2.10
≥15 day	243	0.46	17	4.00	180	0.37	45	1.16
Total	52,910	100.00	425	100.00	48,203	100.00	3,865	100.00

Abbreviation: AEFI=adverse events following immunization.

Causality Assessment of Rare Vaccine Reactions

Among the rare reactions to vaccination, the incidence of allergic reactions was reported as 2.60 per 100,000 doses; specifically, the rates of allergic rash, angioedema, anaphylactic shock, and laryngeal edema were 2.42, 0.10, 0.01, and 0.004 per 100,000 doses, respectively. Reports of nervous system reactions were 0.07 per 100,000 doses, with specific incidences of febrile convulsion, convulsion, Guillain-Barre syndrome (GBS), and acute disseminated encephalomyelitis (ADEM) at 0.05, 0.01, 0.002, and 0.002 per 100,000 doses, respectively. Local reaction rates, which included sterile abscess, Arthus reaction, lymphangitis and lymphadenitis, were recorded as 0.02, 0.01, and 0.003 per 100,000 doses, respectively. Incidences of thrombocytopenic purpura (TP) and Henoch-Schonlein purpura (HSP) were documented at 0.05 and 0.01 per 100,000 doses, respectively (Table 3). Additionally, there were two reported cases of TP in two distinct vaccine batches.

TABLE 2. Number and incidence per 100,000 doses of Hib vaccine AEFI by year, causality, and severity in China, 2010–2021.

Year	Classification by cause												Seriousness				Total	
	Common vaccine reaction		Rare vaccine reaction		Coincidental event		Psychogenic reaction		Immunization error-related reaction		Non-classifiable event		Serious*		Non-serious			
	Number	Incidence (/100,000)	Number	Incidence (/100,000)	Number	Incidence (/100,000)	Number	Incidence (/100,000)	Number	Incidence (/100,000)	Number	Incidence (/100,000)	Number	Incidence (/100,000)	Number	Incidence (/100,000)	Number	Incidence (/100,000)
2010	1,872	16.46	180	1.58	58	0.51	1	0.01	0	0.00	4	0.04	33	0.29	2,082	18.31	2,115	18.60
2011	3,840	26.68	278	1.93	59	0.41	1	0.01	0	0.00	0	0.00	34	0.24	4,144	28.80	4,178	29.03
2012	5,196	37.09	390	2.79	79	0.56	0	0.00	1	0.01	0	0.00	44	0.31	5,622	40.13	5,666	40.44
2013	5,871	40.13	500	3.42	83	0.57	1	0.01	0	0.00	2	0.01	46	0.31	6,411	43.82	6,457	44.14
2014	5,612	36.22	572	3.69	100	0.65	3	0.02	0	0.00	5	0.03	59	0.38	6,233	40.23	6,292	40.61
2015	5,068	32.46	483	3.09	93	0.60	0	0.00	1	0.01	1	0.01	39	0.25	5,607	35.92	5,646	36.17
2016	4,155	40.79	356	3.49	69	0.68	0	0.00	0	0.00	3	0.03	49	0.48	4,534	44.51	4,583	44.99
2017	3,627	32.51	301	2.70	61	0.55	0	0.00	0	0.00	4	0.04	30	0.27	3,963	35.53	3,993	35.79
2018	3,983	38.11	315	3.01	59	0.56	0	0.00	0	0.00	7	0.07	30	0.29	4,334	41.47	4,364	41.75
2019	3,766	46.25	244	3.00	81	0.99	0	0.00	1	0.01	0	0.00	26	0.32	4,066	49.94	4,092	50.25
2020	3,110	45.54	162	2.37	31	0.45	1	0.01	1	0.01	4	0.06	25	0.37	3,284	48.09	3,309	48.46
2021	2,103	31.78	84	1.27	25	0.38	0	0.00	1	0.02	2	0.03	10	0.15	2,205	33.32	2,215	33.47
Total	48,203	34.71	3,865	2.78	798	0.57	7	0.005	5	0.004	32	0.02	425	0.31	52,485	37.79	52,910	38.10

Abbreviation: AEFI=adverse events following immunization.

* Among serious AEFI, there were 224 cases of serious rare vaccine reactions, representing an incidence of 0.16 per 100,000 doses.

TABLE 3. Number, proportion and incidence of reported Hib vaccine reactions in China, 2010–2021.

Clinical diagnosis	Number	Proportion (%)	Incidence (/100,000)
Common vaccine reactions			
Fever (axillary temperature)			
≥38.6 ℃	16,573	34.38	11.93
Injection site redness and swelling (diameter)			
2.6–5.0 cm	10,304	21.38	7.42
> 5.0 cm	3,149	6.53	2.27
Injection site induration (diameter)			
2.6–5.0 cm	3,658	7.59	2.63
> 5.0 cm	1,038	2.15	0.75
Other common vaccine reactions	2,250	4.67	1.62
Rare vaccine reactions			
Allergic reactions			
Allergic rash	3,365	87.06	2.42
Angioedema	142	3.67	0.10
Anaphylactic shock	14	0.36	0.01
Laryngeal edema	5	0.13	0.004
Other allergic reactions	66	1.71	0.05
Nervous system diseases			
Febrile convulsion	71	1.84	0.05
Convulsion	11	0.28	0.01
GBS	3	0.08	0.002
ADEM	3	0.08	0.002
Polyneuritis	2	0.05	0.001
Local reactions			
Sterile abscess	27	0.70	0.02
Arthus reaction	7	0.18	0.01
Lymphangitis and lymphadenitis	4	0.10	0.003
Other rare vaccine reactions			
TP	67	1.73	0.05
HSP	14	0.36	0.01
Others	64	1.66	0.05
Total	52,068	100.00	37.49

Abbreviation: GBS=Guillain-Barre syndrome; ADEM=acute disseminated encephalomyelitis; TP=thrombocytopenic purpura; HSP=Henoch-Schonlein purpura.

The proportions of allergic rash, HSP, TP, febrile convulsion, GBS, polyneuritis, and sterile abscess occurring within three days post-vaccination were 98.16%, 85.71%, 65.67%, 98.59%, 33.33%, 50.00%, and 11.11%, respectively. Additionally, laryngeal edema, ADEM, angioedema, anaphylactic shock, convulsion, and Arthus reactions all occurred within this timeframe following vaccination.

DISCUSSION

The CNIIS serves as the principal platform for AEFI surveillance across Chinese mainland. It compiles comprehensive data on AEFI reports and vaccine doses administered for all post-marketed vaccines, which is pivotal for the quantitative analysis of AEFI. Our study, utilizing data from CNIIS, revealed that AEFIs with the Hib vaccine were more frequently reported in males, within the eastern region, and during the second and third quarters of the year. This distribution mirrors the trend observed in AEFI reports for other vaccines that are market-authorized in China (*4*). Predominantly, AEFIs with the Hib vaccine occurred in infants, aligning with the typical age for Hib

vaccination, and was higher in proportion after the administration of the first dose. Other studies indicate that the AEFI rate was more prevalent following the second and subsequent doses — a trend potentially linked to the cellular immune memory responses (*5*). Additionally, our analysis showed that 25% of Hib vaccine doses were administered concomitantly with other vaccines. The WHO's position paper indicates Hib vaccines are safe and effective when given simultaneously with other vaccines (*1*).

From 2010 to 2021, the incidence of reported AEFI with the Hib vaccine was 38.10 per 100,000 doses. This rate was lower compared to the incidence reported in Australia in 2020, which was 69.4 per 100,000 doses (*6*). Studies conducted in China indicated higher incidences of AEFI for the combined DTP-IPV/Hib vaccine compared to our findings for the standalone Hib vaccine (*4*–*5*,*7*). Our data showed that annual reported incidences ranged from 18.60 to 50.25 per 100,000 doses, with an initially increasing trend that later stabilized. Notably, the highest incidence of AEFI was recorded in 2019, coinciding with an overall increase in AEFI reports for all post-marketed vaccines that year (*8*), possibly due to heightened societal concerns and enhanced surveillance of AEFI. The subsequent decrease in the number and incidence of AEFI reports in 2021 may be attributable to the impact on AEFI surveillance and immunization program services amidst the COVID-19 pandemic. In the same year, the incidence of rare reactions also decreased to 1.27 per 100,000. Furthermore, serious AEFIs were reported at a rate of 0.31 per 100,000 doses, and the incidence of serious rare vaccine reactions (0.16 per 100,000) aligned with the average incidences reported for other vaccines in China (*4*). It is important to note, however, that incidences of AEFI across different countries and regions are not directly comparable due to variations in AEFI reporting systems and methodologies.

The majority (91%) of the AEFI with Hib vaccination were common vaccine reactions. These included local reactions such as redness, swelling, induration, and rash at the injection site, along with systemic reactions such as fever, crying, and vomiting. These findings align with similar observations reported in the United States (*9*) and various regions of China (*5*,*7*). Our analysis indicated that 98% of these common vaccine reactions occurred within three days post-vaccination, consistent with previous national AEFI reports (*4*). Most of these reactions were either effectively managed with treatment or resolved spontaneously.

Allergic reactions were identified as the most commonly reported rare vaccine reactions, exhibiting a reporting rate of 2.60 per 100,000. This rate was significantly lower compared to that observed in the Yinzhou District of Ningbo City, which stands at 18.4 per 100,000 (*10*). Among these, allergic rash accounted for 87% of the cases, with the majority being non-serious, of short duration, and resolving favorably. The reported incidence of angioedema, at 0.10 per 100,000, was slightly higher than the incidence of other vaccines in China (*4*). Cases of anaphylaxis, including manifestations such as anaphylactic shock and laryngeal edema, were exceedingly rare, recorded at 0.01 per 100,000. This incidence was considerably lower than the rates of anaphylaxis reported in the United States, which range from 0.2 to 1.5 per 1,000,000 (*11*–*12*). Most anaphylactic reactions occurred within thirty minutes following vaccination and could pose a life-threatening risk if not promptly managed. Consequently, a post-vaccination observation period of 30 minutes is crucial to timely identify and address any cases of immediate anaphylaxis.

AEFI involving the nervous system are a significant concern post-vaccination. The incidence of nervous system events post-Hib vaccination was reported to be relatively low at 0.07 per 100,000 doses. Febrile convulsions, which generally have a favorable prognosis, emerged as the most common nervous system reaction in our study. These were reported at a rate of 0.05 per 100,000 doses, a figure that aligns with the incidences of similar reactions to other vaccines used in China (*4*) and is notably lower than the rate of febrile convulsions following the DPT-IPV/Hib vaccine in Zhejiang province, which stands at 0.50 per 100,000. The incidence of other neurological events such as GBS and ADEM was exceedingly rare, not exceeding 0.01 per 100,000 doses. Furthermore, no causal link has been established between these neurological conditions and the Hib vaccine. Based on these findings, we advocate for the continuation of vigilant neurological event surveillance following Hib vaccination.

Other rare vaccine reactions have also been reported. In our study, the incidence of TP was 0.05 per 100,000 doses, aligning with the average incidence reported for other vaccines in China (*4*). Comparatively, a survey in France examining TP cases among individuals under 18 years from 2009 to 2011 identified an incidence of 2.9 per 100,000 person-years, with the highest incidence occurring between ages 1 and 5 (*13*). However, the diagnostic criteria for TP differ between China and other countries,

complicating direct comparisons. The incidence of HSP with Hib vaccine in our study was 0.01 per 100,000, slightly lower than the average incidence observed across other vaccines in China (*4*). Meanwhile, studies in Sweden and France indicated an annual incidence of HSP in children under 15 years of age ranging from 17.5 to 30 per 100,000 doses (*14*–*15*). The WHO position paper on the Hib vaccine has not identified any safety concerns (*1*).

This study is subject to some limitations. Passive surveillance systems, such as the one used in this research, are inherently vulnerable to underreporting. Additionally, inaccuracies in data entry and variations in the quality of causality assessments, particularly for non-NIP vaccines, may affect the reliability of our findings. Furthermore, we were unable to ascertain the incidence of AEFI among different subgroups due to the lack of available data regarding the number of Hib vaccine doses administered to these subgroups. Our analysis was also confined to the evaluation of AEFI with monovalent Hib vaccines, thereby excluding combination vaccines from our study. Despite these limitations, the extensive administration of monovalent Hib vaccine doses across China lends substantial support to the robustness of our safety evaluation for this vaccine.

In conclusion, the predominant adverse reactions with the Hib vaccine included fever, injection site reactions, and other common vaccine-related symptoms. The incidence of rare adverse reactions was exceedingly low, primarily consisting of allergic rashes. Serious reactions were extremely uncommon. It is imperative to conduct AEFI surveillance and improve the quality of reporting systems. The favorable safety profile of the Hib vaccine advocates for its broader implementation in China.

Conflicts of interest: No conflicts of interest.

Acknowledgements: The staff at the provincial, prefectural, and county CDCs, as well as all the vaccination clinics involved in conducting the adverse event surveillance. Also, Lance Rodewald, senior consultant at China CDC, for his insightful comments and recommendations on the manuscript.

Funding: Supported by the Emergency Response Mechanism Operation Programme of China CDC (102393220020010000017).

doi: 10.46234/ccdcw2024.180

[#] Corresponding author: Keli Li, likl@chinacdc.cn.

[1] National Key Laboratory of Intelligent Tracking and Forecasting for Infectious Diseases (NITFID), National Immunization Programme, Chinese Center for Disease Control and Prevention, Beijing, China; [2] Department of Expanded Programme on Immunization, Hangzhou Center for Disease Control and Prevention, Hangzhou City, Zhejiang Province, China.

Submitted: April 03, 2024; Accepted: June 26, 2024

REFERENCES

1. World Health Organization. WHO position papers on Haemophilus influenzae type b. 2022. https://www.who.int/teams/immunization-vaccines-and-biologicals/policies/position-papers/haemophilus-influenzae-type-b. [2024-2-2].
2. Ministry of Health of China, State Food and Drug Administration of China. National guideline for the surveillance of adverse events following immunization (AEFI). 2010. http://www.nhc.gov.cn/jkj/s3581/201402/5dd5633d93174a7c8e93d8af7579a613.shtml. [2023-1-10]. (In Chinese).
3. Ministry of Health of China. Identification of adverse reaction after immunization. 2018. http://www.nhc.gov.cn/fzs/s3576/201808/e4f7a5704a994a14bd28cd82f94d27e2.shtml. [2023-1-10]. (In Chinese).
4. Zhang LN, Li KL, Li Y, Fan CX, Li Y, Ren MR, et al. Surveillance of adverse events following immunization in China, 2020. Chin J Vaccines Immun 2022;28(2):208 – 18 https://doi.org/10.19914/j.CJVI.2022041. (in Chinese).
5. Li ZQ, Xu JX, Tan HF, Zhang CH, Chen J, Ni LH, et al. Safety of pentavalent DTaP-IPV/Hib combination vaccine in post-marketing surveillance in Guangzhou, China, from 2011 to 2017. Int J Infect Dis 2020;99:149 – 55. https://doi.org/10.1016/j.ijid.2020.07.019.
6. Dey A, Wang H, Quinn H, Pillsbury A, Hickie M, Deng L, et al. Surveillance of adverse events following immunisation in Australia annual report, 2020. Commun Dis Intell (2018) 2022;46:1-26. http://dx.doi.org/10.33321/cdi.2022.46.47.
7. Pan XJ, Lv HK, Liang H, Wang Y, Shen LZ, Chen FX, et al. Surveillance on the adverse events following immunization with the pentavalent vaccine in Zhejiang, China. Hum Vaccin Immunother 2022;18(1):2021711. https://doi.org/10.1080/21645515.2021.2021711.
8. Zhang LN, Li KL, Du W, Li Y, Fan CX, Yu WZ, et al. Surveillance of adverse events following immunization in China, 2019. Chin J Vaccines Immun 2021;27(4):438 – 45. https://doi.org/10.19914/j.CJVI.2021075. (in Chinese).
9. Moro PL, Jankosky C, Menschik D, Lewis P, Duffy J, Stewart B, et al. Adverse events following *Haemophilus influenzae* type b vaccines in the vaccine adverse event reporting system, 1990-2013. J Pediatr 2015;166(4):992 – 7. https://doi.org/10.1016/j.jpeds.2014.12.014.
10. Huang K, Tao S, Zhou XF, Mo JP, Zhu BW, Shen P, et al. Incidence rates of health outcomes of interest among Chinese children exposed to selected vaccines in Yinzhou Electronic Health Records: a population-based retrospective cohort study. Vaccine 2020;38(18):3422 – 8. https://doi.org/10.1016/j.vaccine.2020.03.013.
11. Su JR, Moro PL, Ng CS, Lewis PW, Said MA, Cano MV. Anaphylaxis after vaccination reported to the vaccine adverse event reporting system, 1990-2016. J Allergy Clin Immunol 2019;143(4):1465 – 73. https://doi.org/10.1016/j.jaci.2018.12.1003.
12. Bohlke K, Davis RL, Marcy SM, Braun MM, DeStefano F, Black SB, et al. Risk of anaphylaxis after vaccination of children and adolescents. Pediatrics 2003;112(4):815 – 20. https://doi.org/10.1542/peds.112.4.815.
13. Moulis G, Palmaro A, Montastruc JL, Godeau B, Lapeyre-Mestre M, Sailler L. Epidemiology of incident immune thrombocytopenia: a nationwide population-based study in France. Blood 2014;124(22):3308 – 15. https://doi.org/10.1182/blood-2014-05-578336.
14. Mossberg M, Segelmark M, Kahn R, Englund M, Mohammad AJ. Epidemiology of primary systemic vasculitis in children: a population-based study from southern Sweden. Scand J Rheumatol 2018;47(4):295 – 302. https://doi.org/10.1080/03009742.2017.1412497.
15. Piram M, Maldini C, Biscardi S, De Suremain N, Orzechowski C, Georget E, et al. Incidence of IgA vasculitis in children estimated by four-source capture-recapture analysis: a population-based study. Rheumatology (Oxford) 2017;56(8):1358 – 66. https://doi.org/10.1093/rheumatology/kex158.

Preplanned Studies

Risk Factors for Norovirus Outbreaks in Schools and Kindergartens — Beijing Municipality, China, July 2017–June 2022

Baiwei Liu[1]; Yu Wang[1]; Mengdi Tan[2]; Boran E[3]; Dongxue Zhang[4]; Hanqiu Yan[1]; Quanyi Wang[1]; Daitao Zhang[1]; Lei Jia[1,#]; Zhiyong Gao[1,2,#]

Summary

What is already known on this topic?

Norovirus is the leading cause of global acute gastroenteritis outbreaks. Norovirus outbreaks mainly occur in schools and kindergartens in China, always causing public health issues.

What is added by this report?

Conditional logistic regression method was used to analyze the risk factors for norovirus outbreaks in schools and kindergartens, and found that students vomiting at school or kindergarten, case activity in public areas, and the first case's classroom less than 5 meters from toilets were risk factors.

What are the implications for public health practice?

Effective measures to address these factors can help reduce the risk of norovirus outbreaks in schools and kindergartens.

Norovirus is the most common cause of acute gastroenteritis outbreaks worldwide (*1*). In China and some other Asian countries, most norovirus outbreaks occur in schools and kindergartens (*2*). Norovirus infection is difficult to control in these enclosed and crowded settings, which can easily lead to outbreaks of gastroenteritis (*3*). There are few studies on the risk factors of norovirus outbreaks in schools and kindergartens (*4*–*6*). This study analyzed the impact of facility conditions, disinfection procedures, and case activities on norovirus outbreaks in schools and kindergartens. Norovirus outbreaks were defined as the case group, and a 1∶2 matching approach was applied to select a control group with norovirus clusters. Univariate and multivariate conditional logistical regression analyses showed that students vomiting at school or kindergarten, case activity in public areas, and first case's classroom less than 5 meters from toilets were risk factors for norovirus outbreaks. Taking targeted measures to reduce or eliminate the impact of these factors will help control norovirus outbreaks in schools and kindergartens.

Primary, secondary, and kindergarten schools in Beijing Municipality, China that reported norovirus clusters or outbreaks between July 2017 and June 2022 were selected for this study. Trained professionals conducted epidemiological investigations, collecting anal swabs or stool samples for nucleic acid detection, and a norovirus outbreak was confirmed if more than two cases tested positive for norovirus. Referring to the guidelines on outbreak investigation, prevention, and control of norovirus infection (*7*), an outbreak was defined as 20 or more epidemiologically linked cases occurring in a collective unit within 7 days. A cluster was defined as 3 or more epidemiologically linked cases occurring in a collective unit within 3 days, that did not meet the outbreak criteria. Outbreaks were used as the case group and were matched 1∶2 with clusters as the control group. In this study, a surveillance year started on July 1 and ended on June 30 of the following year. The urban area of Beijing includes Dongcheng, Xicheng, Chaoyang, Haidian, Fengtai, and Shijingshan districts. The suburbs include Changping, Daxing, Shunyi, Tongzhou, Jingkai, Fangshan, Mentougou, Huairou, Miyun, Pinggu, and Yanqing districts.

This study constructed a database using WPS Spreadsheets 2016 (Kingsoft Inc., Beijing, China) and performed statistical analyses using SPSS software (version 19.0, IBM, Chicago, IL, USA). The median, interquartile range (IQR), and composition ratio described the epidemiological characteristics of norovirus clusters and outbreaks. The timeliness of reporting refers to the interval between the onset time of the first case and the reporting time of norovirus clusters or outbreaks. Chi-square tests compared the epidemiological characteristics between norovirus clusters and outbreaks. After case-control matching,

risk factors were assessed using univariate conditional logistic regression. Variables with $P<0.1$ were included in the multivariate conditional logistic regression analyses, and $P<0.05$ were considered statistically significant.

From July 2017 to June 2022, a total of 1,281 norovirus clusters and outbreaks were reported in Beijing, most of them (92.12%, 1,180/1,281) occurred in primary, secondary, and kindergarten schools, and most (98.56%, 1,163/1,180) were caused by person-to-person transmission. The 1,163 norovirus clusters and outbreaks of person-to-person transmission were included in the study, which involved all 17 districts of Beijing, and 73 (6.28%) of which were outbreaks. The median number of cases per cluster or outbreak was 8 (IQR 5-12), with a maximum of 156 cases. A total of 661 (56.84%) norovirus clusters and outbreaks occurred in kindergartens, and 43.16% (502/1,163) occurred in primary and secondary schools. The majority (82.54%, 960/1,163) were caused by GII genogroup noroviruses, 12.30% (143/1,163) by GI genogroup noroviruses, 2.84% (33/1,163) by co-infection of GI and GII genogroups, 2.15% (25/1,163) by co-infection of noroviruses and other viruses, and 0.17% (2/1,163) by noroviruses of unknown genogroup.

Epidemiological characteristics were compared between norovirus clusters and outbreaks, the timeliness of reporting for both norovirus clusters and outbreaks was 2 (IQR 1-3) days, and there was no significant difference between them ($Z=-0.725$, $P=0.468$). Statistically significant differences were found in the proportion by year (July 2017 to June 2022), school type (kindergarten and school), and region (urban and suburban) (Table 1). To exclude the impact of these external factors on norovirus outbreaks in schools and kindergartens, a 1∶2 match was used for occurrence times (every two months), school types, and regions. Seventy outbreaks and 134 clusters were successfully matched.

This study analyzed three types of internal factors in schools and kindergartens: facility conditions, disinfection measures, and the activities of cases (Table 2). Univariate factor conditional logistic regression analysis showed that 7 of the 12 factors were statistically significant ($P<0.1$): water supply, distance between the first case's classroom and toilet, daily disinfection concentration, standard handling of vomit, case activity in public areas, vomiting site of the first case, and students vomiting at school or kindergarten. These seven factors were incorporated into a multivariate conditional logistic regression. The results showed that the risk of norovirus outbreaks was 18.63 times higher for students who vomited at school

TABLE 1. Comparison of epidemiological characteristics between norovirus outbreaks and clusters in Beijing Municipality, China, July 2017–June 2022.

Characteristics	Outbreaks (*N*=73)	Clusters (*N*=1,090)	χ^2	*P*
	n (%)	*n* (%)		
Year			38.244	<0.001
July 2017−June 2018	18 (24.66)	133 (12.20)		
July 2018−June 2019	35 (47.94)	272 (24.95)		
July 2019−June 2020	7 (9.59)	125 (11.47)		
July 2020−June 2021	10 (13.70)	342 (31.38)		
July 2021−June 2022	3 (4.11)	218 (20.00)		
School type			30.135	<0.001
Primary and secondary schools	54 (73.97)	448 (41.10)		
Kindergartens	19 (26.03)	642 (58.90)		
Region			6.113	0.013
Urban	33 (45.21)	653 (59.91)		
Suburb	40 (54.79)	437 (40.09)		
Pathogen type				
Only norovirus	69 (94.52)	1,069 (98.07)		0.066*
Norovirus mixed with other viruses	4 (5.48)	21 (1.93)		

* Fisher test.

TABLE 2. The risk factors for norovirus outbreaks in schools and kindergartens in Beijing Municipality, China, July 2017–June 2022.

Factors	Outbreaks	Clusters	Univariate analysis		Multivariate analysis	
	(*N*=70)	(*N*=134)	*OR* (95% *CI*)	*P*	*OR* (95% *CI*)	*P*
Facility conditions						
Property of schools or kindergartens						
Public or registered	61	121	Reference			
Private or unregistered	9	13	1.46 (0.59−3.62)	0.420		
Water supply						
Municipal	62	130	Reference		Reference	
Self-harvesting or others	8	4	3.80 (1.14−12.68)	0.030*	2.68 (0.52−13.79)	0.238
Dining						
Food delivery or self-catering	15	31	Reference			
Canteen	55	102	1.12 (0.55−2.18)	0.763		
Classroom lighting						
Non-south or indirect	13	28	Reference			
South or direct	57	106	1.19 (0.56−2.53)	0.658		
Classroom ventilation						
≥3 times/day	44	89	Reference			
<3 times/day	26	45	1.07 (0.52−2.20)	0.854		
Distance between the first cases' classroom and toilet						
>5 m	31	72	Reference		Reference	
0−5 m	34	51	2.13 (0.98−4.64)	0.057*	3.19 (1.15−8.82)	0.025†
Disinfection measures						
Daily disinfection concentration						
≥500 mg/L	24	66	Reference		Reference	
<500 mg/L	45	64	2.51 (1.27−4.97)	0.008*	1.79 (0.67−4.81)	0.249
Partition usage of cleaning tools						
Yes	68	132	Reference			
No	2	2	2.00 (0.28−14.20)	0.488		
Standard handling of vomit						
Yes	36	78	Reference		Reference	
No	30	38	1.84 (0.90−3.75)	0.094*	1.01 (0.40−2.54)	0.983
Activities of cases						
Cases activity in public areas						
No	38	88	Reference		Reference	
Yes	32	45	1.70 (0.94−3.08)	0.078*	3.46 (1.29−9.26)	0.014†
Vomiting site of the first case						
Home	26	79	Reference		Reference	
School	44	55	2.37 (1.30−4.32)	0.005*	1.87 (0.80−4.39)	0.151
Students vomiting at school or kindergarten						
No	5	41	Reference		Reference	
Yes	65	93	7.85 (2.35−26.27)	0.001*	18.63 (1.89−184.10)	0.012†

Note: Standard handling of vomit: evacuate students from the vomiting area as soon as possible, open windows for ventilation, wear personal protective equipment, disinfect the vomit with chlorine-containing preparations, and then remove the vomit and clean the floor, and at last, wipe them with clean water. Partition usage of cleaning tools: different tools for classrooms, corridors and toilets. Public area: public classrooms and playgrounds in schools and kindergartens.
Abbreviation: *OR*=odds ratio; *CI*=confidence interval.
* *P*<0.1;
† *P*<0.05.

or kindergarten than for students who did not [95% confidence interval (*CI*): 1.89, 184.10], 3.46 times higher for cases that involved activity in public areas than for cases that involved staying in the classroom or going home on time (95% *CI*: 1.29, 9.26), and 3.19 times higher for the first case's classrooms less than 5 meters from toilets than for classrooms more than 5 meters from toilets (95% *CI*: 1.15, 8.82) (Table 2).

DISCUSSION

From 2007 to 2021, norovirus outbreaks in China showed an overall increasing trend, with 89.22% occurring in schools and kindergartens (*8*). Therefore, there is a need to improve prevention and control measures in these settings. Studies on risk factors for norovirus outbreaks conducted outside of China have mostly focused on medical institutions (*6*). In China, two studies found that school types, region, and hand hygiene can affect the scale of norovirus outbreaks (*4*–*5*). However, few studies have focused on various internal factors in schools and kindergartens. This study used conditional logistic regression to analyze the risk factors for norovirus outbreaks and identified several key factors: students vomiting at school or kindergarten, case activity in public areas, and the first case's classroom less than 5 meters from toilets. Norovirus outbreaks in schools or kindergartens in Beijing appear to be mainly influenced by the activities of cases. Effective measures to address these risk factors can help control norovirus outbreaks in schools and kindergartens.

Norovirus is typically excreted in feces. One study demonstrated that murine norovirus can be aerosolized when toilets are flushed (*9*). The feces of infected individuals can directly contaminate the environment and produce norovirus aerosols during defecation and flushing. This study found that when the first cases' classroom was near a toilet, students from nearby classrooms were more likely to contact norovirus aerosols and contaminated environments, increasing their norovirus exposure and accelerating disease spread. Therefore, timely toilet disinfection and ventilation are critical. Vomiting in classrooms, toilets, and corridors can contaminate the surrounding environment and generate norovirus aerosols. Wanwan Sun et al. found that the odds ratio (*OR*) of norovirus infection among teachers who handled student vomit without respiratory protection was 15.75 times that of teachers without this exposure (*10*). Therefore, standard vomit disposal is critical for reducing norovirus outbreaks. Patient isolation is an effective means of preventing pathogen spread. If students remain active in common areas of schools and kindergartens after illness onset, more people will be at risk of exposure. Once someone falls ill, immediate isolation measures should be taken until three days after symptom resolution.

This study was subject to some limitations. First, this study only analyzed 12 factors in schools and kindergartens, without incorporating factors such as the timeliness of detection, the standardization of case management and transmission modes. Second, norovirus genotypes were not included in this study. Differences in the transmissibility of different norovirus genotypes may affect the occurrence of norovirus outbreaks.

If a norovirus cluster or outbreak occurs in a school or kindergarten, increasing the frequency of toilet disinfection, ensuring the timely and correct disposal of vomit, and immediately isolating cases will help control its scale, prevent further infection, and reduce the burden of disease.

Conflicts of interest: No conflicts of interest.

Acknowledgements: We thank the staff of the district Center for Disease Prevention and Control in Beijing for performing epidemiological investigation and laboratory detection.

Funding: Supported by National Key R&D Programme of China (2021ZD0114103), Capital's Funds for Health Improvement and Research (2022-1G-3014) and High-level Public Health Technical Talents Construction Project (Academic Leader 02-07).

doi: 10.46234/ccdcw2024.181

[#] Corresponding authors: Lei Jia, Lailajia@126.com; Zhiyong Gao, zhiyonggao1@163.com.

[1] Institute for Infectious Disease and Endemic Disease Control, Beijing Center for Disease Prevention and Control, Beijing, China; [2] School of Public Health, China Medical University, Shenyang City, Liaoning Province, China; [3] School of Public Health, Capital Medical University, Beijing, China; [4] Department of Endocrinology, Beijing Shijitan Hospital, Capital Medical University, Beijing, China.

Submitted: January 05, 2024; Accepted: August 02, 2024

REFERENCES

1. Khan MK, Alam MM. Norovirus gastroenteritis outbreaks, genomic diversity and evolution: an overview. Mymensingh Med J 2021;30(3): 863-73. https://pubmed.ncbi.nlm.nih.gov/34226482/.
2. Jin M, Wu SY, Kong XY, Xie HP, Fu JG, He YQ, et al. Norovirus outbreak surveillance, China, 2016-2018. Emerg Infect Dis 2020;26(3): 437 – 45. https://doi.org/10.3201/eid2603.191183.

3. Harris JP, Lopman BA, O'Brien SJ. Infection control measures for norovirus: a systematic review of outbreaks in semi-enclosed settings. J Hosp Infect 2010;74(1):1 – 9. https://doi.org/10.1016/j.jhin.2009.07.025.
4. Liu BW, Gao ZY, Jia L, Yan HQ, Wang XL, Zhang XX, et al. Analysis on influencing factors for acute gastroenteritis outbreaks caused by norovirus in Beijing, 2014-2018. Chin J Epidemiol 2019;40(10):1274 – 8. https://doi.org/10.3760/cma.j.issn.0254-6450.2019.10.019.
5. Dai YX, Su LY, Liu YS, Chen H, Yue Y, Han DL. Distribution of norovirus outbreaks and associated factors in Chengdu during 2017. Chin J Sch Health 2019;40(1):107 – 9. https://doi.org/10.16835/j.cnki.1000-9817.2019.01.029.
6. Fraenkel CJ, Inghammar M, Söderlund-Strand A, Johansson PJH, Böttiger B. Risk factors for hospital norovirus outbreaks: impact of vomiting, genotype, and multi-occupancy rooms. J Hosp Infect 2018;98(4):398 – 403. https://doi.org/10.1016/j.jhin.2018.01.011.
7. Liao QH, Ran L, Jin M, Cui SH, Yuan J, Ma HL, et al. Guidelines on outbreak investigation, prevention and control of norovirus infection (2015). Chin J Prev Med 2016;50(1):7 – 16. https://doi.org/10.3760/cma.j.issn.0253-9624.2016.01.003.
8. Tang QY, Gao XY, Song Y, Zhang YT, Ran L, Chang ZR, et al. Epidemiological characteristics of norovirus acute gastroenteritis outbreaks and influencing factors in China, 2007-2021. Chin J Epidemiol 2023;44(5):751 – 8. https://doi.org/10.3760/cma.j.cn112338-20221109-00956.
9. Boles C, Brown G, Nonnenmann M. Determination of murine norovirus aerosol concentration during toilet flushing. Sci Rep 2021;11(1):23558. https://doi.org/10.1038/s41598-021-02938-0.
10. Sun WW, Pang ZF, He YY, Chen YJ, Pan JR, Gao J, et al. Improper handling of vomitus as a risk factor in the human norovirus outbreak in a kindergarten in Wuyi County, Zhejiang Province, China. Epidemiol Infect 2022;150:e111. https://doi.org/10.1017/s0950268822000826.

Preplanned Studies

Infection and Genomic Characteristics of *Campylobacter jejuni* from a Patient Without Diarrhea — China, 2018

Xiangdong Yang[1,2]; Wen Wang[1]; Chajin Cui[3]; Binbin Yu[2]; Qing Zhang[2]; Yanhua Wang[1,#]

Summary

What is already known about this topic?

A 20-month-old boy was admitted to the hospital with a maximum temperature of 40 °C and a single convulsion. Unexpectedly, blood culture detected *Francisella tularensis* (*F. tularensis*) using the VITEK 2 Compact System.

What is added by this report?

After incubation of the patient's blood for 48 hours, the cultured strain was identified as *Campylobacter jejuni*, named L8, excluding *F. tularensis*. In the genome sequence of L8, we found a novel Type VI Secretion System (T6SS), of which the conserved C-terminal VgrG domain from positions 561 to 884 showed significant changes.

What are the implications for public health practice?

It should be underscored that relying solely on automatic bacterial identification instruments for accurate strain identification is unreliable. Moreover, our study suggests that the potential effect of T6SS should be considered when studying the genetic features of a patient's clinical phenotypes.

Campylobacter jejuni (*C. jejuni*) is widely recognized as the primary causative agent of global foodborne bacterial diarrheal disease (*1*). Despite a limited number of documented *C. jejuni* outbreaks in China (*2*), a young patient in Yunnan Province presented with suspected tularemia. The patient presented with high fever and convulsions rather than typical diarrheal symptoms, but the isolated strain was biochemically identified as *C. jejuni*.

To elucidate the genetic features contributing to the clinical phenotype in this case, the isolate underwent comprehensive whole-genome sequencing. This investigation aimed to discern the genetic relationships between this strain and previously sequenced *C. jejuni* strains, considering population structure, differences in genomic composition, and common virulence factors in comparison to reference strains. Additionally, the presence of specific virulence factors was investigated. Furthermore, 13 major components of the Type VI Secretion System (T6SS) and *Campylobacter jejuni* Integrated Element 3 (CJIE3) were identified and analyzed.

A 20-month-old boy was admitted to the hospital with a maximum temperature of 40 °C, which had fluctuated around 39 °C for eight hours prior. The patient exhibited no respiratory or gastrointestinal symptoms but experienced a single, one-minute convulsion five minutes prior to admission, after which he regained consciousness. The initial diagnosis was herpes pharyngitis with febrile convulsions. The patient had no history of infection. His white blood cell count was within the normal range at 10.8×10^9/L (with elevated neutrophils at 78.1% and decreased lymphocytes at 14.0%). Hypersensitive C-reactive protein levels were elevated at 41.5 mg/L. Procalcitoninogen and erythrocyte sedimentation rate were both within normal limits at 0.134 ng/mL and 11 mm/h, respectively. Electroencephalogram and digital computed tomography scan of the head and lungs revealed no abnormalities. Unexpectedly, blood culture detected *Francisella tularensis* using the VITEK 2 Compact System based on the positive PyrA. Intracranial infection and central nervous system disease were ruled out based on the patient's signs and symptoms and clinical test results. The study was approved by the Ethics Committee of the Yunnan Institute of Endemic Diseases Control & Prevention (Ethics Committee approval number 2021-09). Informed consent was obtained from legal guardians.

In the reported clinical case of suspected tularemia, blood was inoculated onto cysteine heart agar blood plates suitable for *F. tularensis* in a 5% CO_2 incubator at 37 °C. After 48 hours of incubation, the culture medium exhibited several single colonies, 1–2 mm in diameter, with a teardrop shape and consistent morphology. Tularemia was ruled out in this patient based on negative tests for *F. tularensis*-specific antigens and antibodies. The colonies were Gram-stain-negative and elongated in an S-shape without spores, and all

were identified as *C. jejuni* through positive reactions for oxidase, catalase, and hippurate hydrolysis. One strain was selected for high-quality whole-genome sequencing and confirmed as *C. jejuni*. This strain, designated L8, was tested for susceptibility to 12 antibiotics. The results showed that L8 was resistant to ciprofloxacin and tetracycline and sensitive to the other antibiotics. Comparisons using ResFinder (https://cge.food.dtu.dk/services/ResFinder/) and CARD (https://card.mcmaster.ca/analyze), a database of drug resistance genes, revealed that L8 expressed *cmeABC* and *cmeR*, which are closely related to macrolide, fluoroquinolone, cephalosporin, and fusidane resistance. The tetracycline, doxycycline, and minocycline resistance gene *tet(O)* was also expressed.

The *C. jejuni* L8 genome was completely sequenced (GenBank accession no. CP139640) and comprised a single contig of 1,732,398 bp with no plasmids (Figure 1A). The L8 genome exhibited a G+C content of 30.29% and an ANI of 98.44%. Although L8 shared similar genomic characteristics with NCTC 11168, collinear analyses indicated that L8 possessed an additional fragment of 93,816 bp (Figures 1C, 1D), housing approximately 90 more genes, of which 55 had functional annotations (Supplementary Table S1, available at https://weekly.

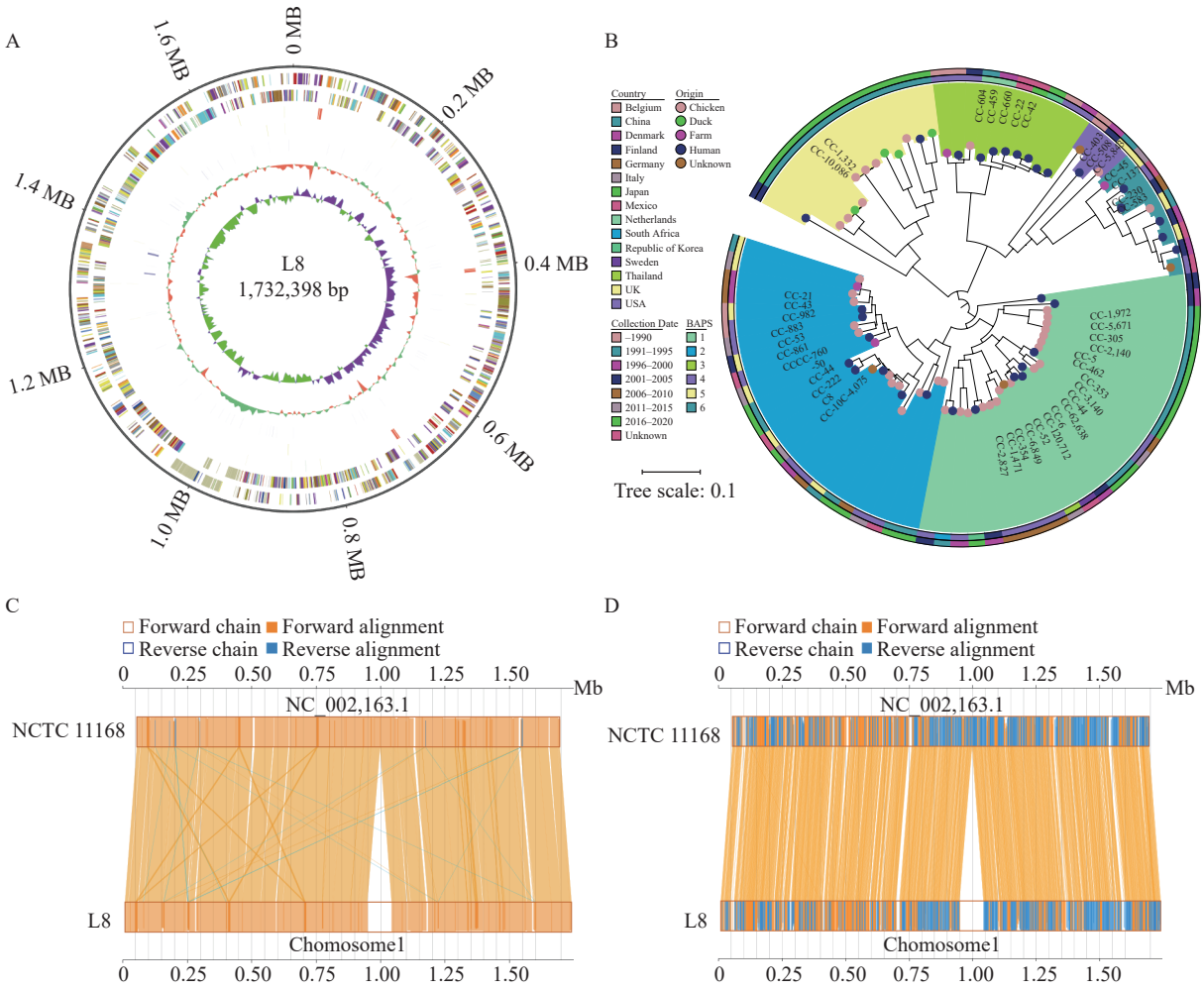

FIGURE 1. Complete genomes of *C. jejuni* L8, comparative genomic analysis with NCTC 11168, and population structure of 84 *C. jejuni* strains based on the core genome alignment with BAPS clusters. (A) Circular representation of the chromosome from *C. jejuni* L8. (B) Population structure of 84 C. jejuni strains based on the core genome alignment with BAPS clusters. (C) Co-linear analysis of the genome between C. jejuni L8 and C. jejuni NCTC 11168 using MUMmer. (D) Co-linear analysis of the proteome between *C. jejuni* L8 and *C. jejuni* NCTC 11168 using MUMmer.

Note: In panel B, the clonal complexes are color-coded in the inner ring; the country of genome origin is coded in the second ring; and the collection date of the genome is described in the outer ring. The leaves are colored by the origin of each sample. In panel C, the yellow connecting lines in the middle region indicate high sequence identity of the forward alignment, and the blue lines represent the reverse complementary alignment.

chinacdc.cn).

The 84 *C. jejuni* genomes, including L8, were isolated from poultry, human, and environmental samples from various countries. These genomes comprised 600 core genes, covering 54.6% of the average genome size of 1,694,827 bp. Phylogenetic analysis revealed six distinct branches (*1*–*6*), confirmed by BAPS clustering (Figure 1B). These branches were characterized by their clonal complexes (CCs), sequence type, geographic location, isolation source, and collection year (Supplementary Table S2, available at https://weekly.chinacdc.cn/). L8 belonged to sequence type ST-464, assigned to BAPS cluster 1, which included isolates from eight countries. A total of 126 common virulence genes and 83 shared virulence factors were identified in L8, NCTC 11168, RM 1221, and 81-176, representing the fundamental elements contributing to *C. jejuni* virulence (Figure 2A). The distribution of virulence factors was most similar between L8 and NCTC 11168. L8 harbored 27 virulence genes, exhibiting the greatest diversity compared to 81-176 (15 virulence genes), excluding RM 1221, which contained the fewest virulence factors (Figure 2B). The previously identified virulence factor CDT was present in L8. Phylogenetic analysis of the *cdtA* gene indicated significant differences in L8 compared to other strains (Figure 3, *cdtA*), although no distinct variations were observed for *cdtB* and *cdtC* (Figure 3, *cdtB*, *cdtC*). Additionally, other virulence traits, such as lipooligosaccharide sialylation and the metabolism-related virulence factors γ-glutamyl transpeptidase (GGT) and fucose permease (Cj0486), were absent in L8.

Strain L8 harbored the 13 T6SS core components. Comparisons with T6SS-positive *C. jejuni* 108 and 488 revealed a strongly conserved T6SS cluster, sharing synteny in the genomic arrangement among *C. jejuni* strains (Figure 4A). In L8, the C-terminal *tssI* (*vgrG*) domain from positions 561 to 884 differed observably from those in 108 and 488. Notably, in L8, 25 amino acids were inserted at positions 566 to 590 and 16 amino acids at positions 596 to 611, respectively (Figure 4C). In contrast, the amino acid sequences at the same positions of 108 and 488 showed high consistency of 99.38%. Furthermore, L8 exhibited consecutive or scattered mutations outside of the two insertion segments from 561 to 884. Additionally, CJIE3 was identified in L8.

DISCUSSION

Here, we isolated strain L8 from a clinically reported case of suspected tularemia and identified it as *C. jejuni* through biochemical characteristics and whole-genome

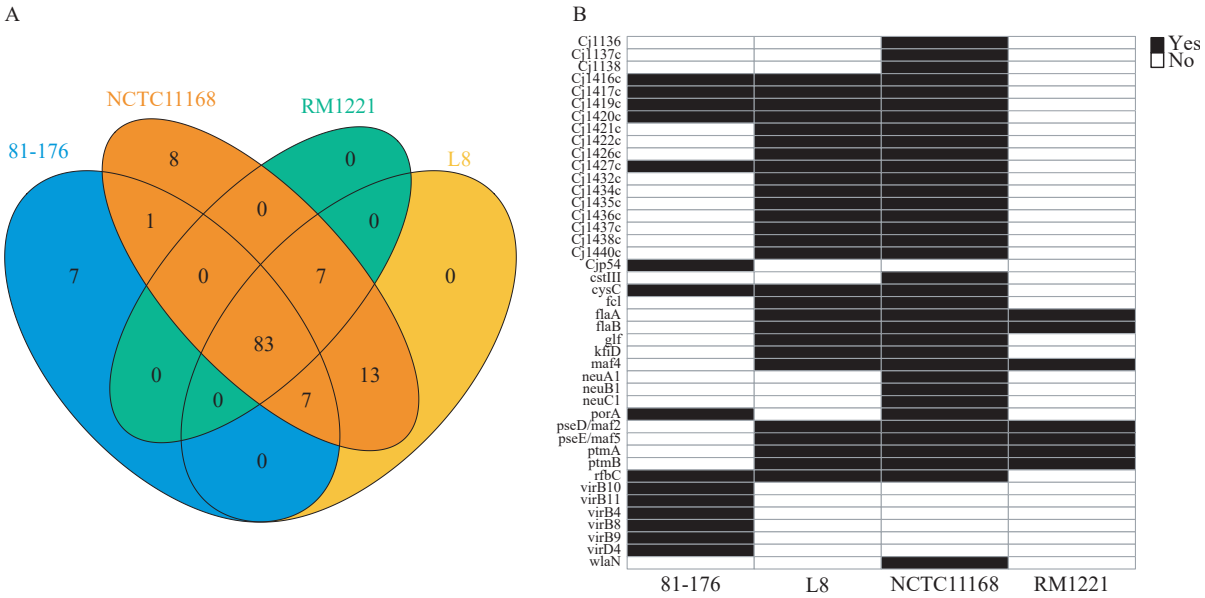

FIGURE 2. Distribution comparison of 126 virulence genes in the four strains. (A) Venn diagram of the relationship between the 126 genes identified in the four strains. (B) Heat map of the distribution of the remaining 43 virulence factors except the 83 shared.
Note: A total of 98, 119, 90, and 110 genes were detected in *C. jejuni* 81-176, NCTC 11168, RM 1221, and L8, respectively. L8 shared 110 genes with NCTC 11168, 90 genes with RM 1221, and 90 genes with 81-176.

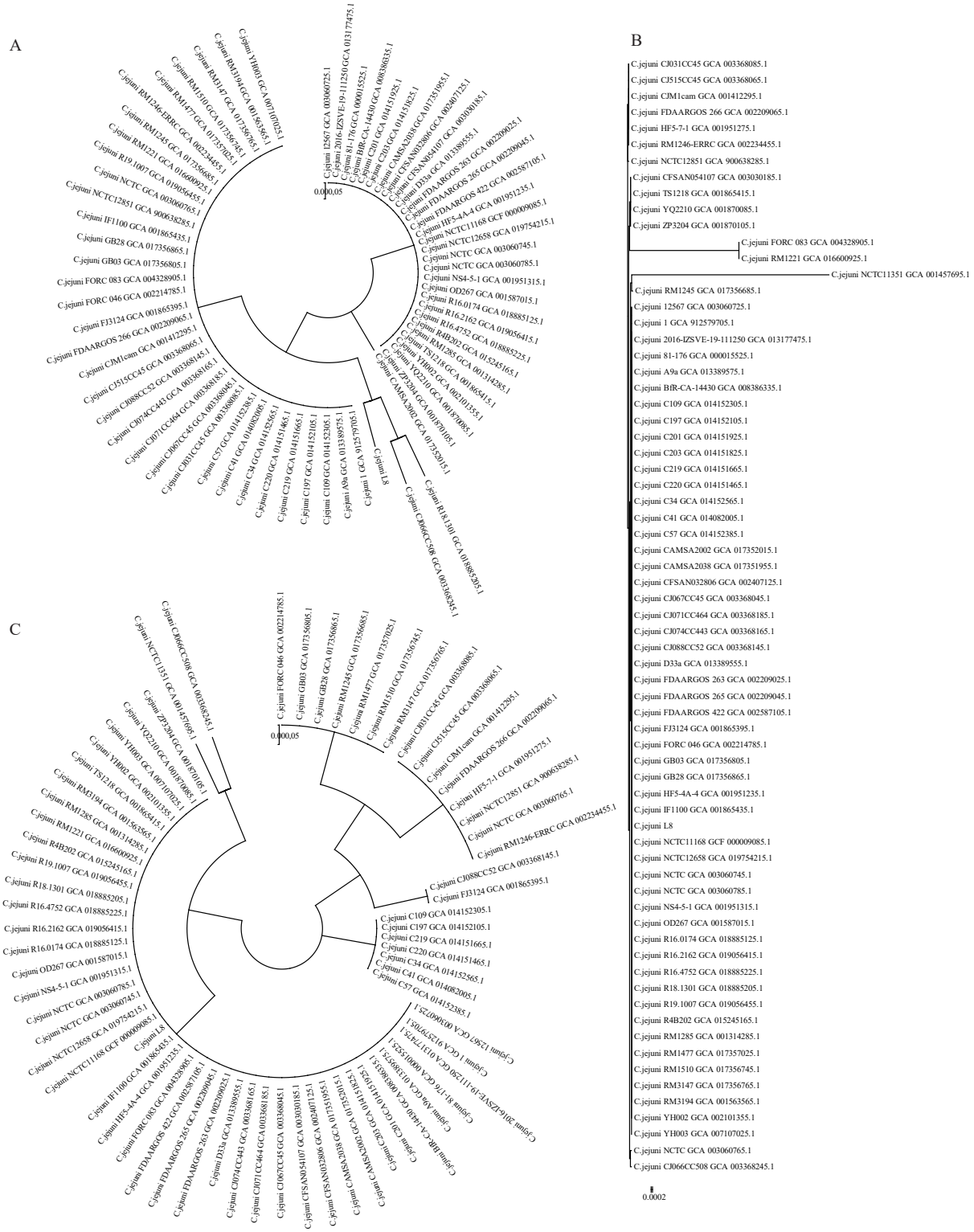

FIGURE 3. Phylogenetic tree of predicted amino acid sequence variants encoded by (A) *cdtA*, (B) *cdtB*, and (C) *cdtC* in the 84 *C. jejuni* strains from different geographic backgrounds.
Note: CdtA was predicted in 67 of the 84 *C. jejuni* strains, and both CdtB and CdtC in 69. The L8 strain is denoted with a black triangle.

sequencing. Genomic comparisons revealed the presence of a T6SS-containing CJIE3 in L8, considered a novel variant of the pathogenicity island (*3*). Notably, the insertion of two long segments and

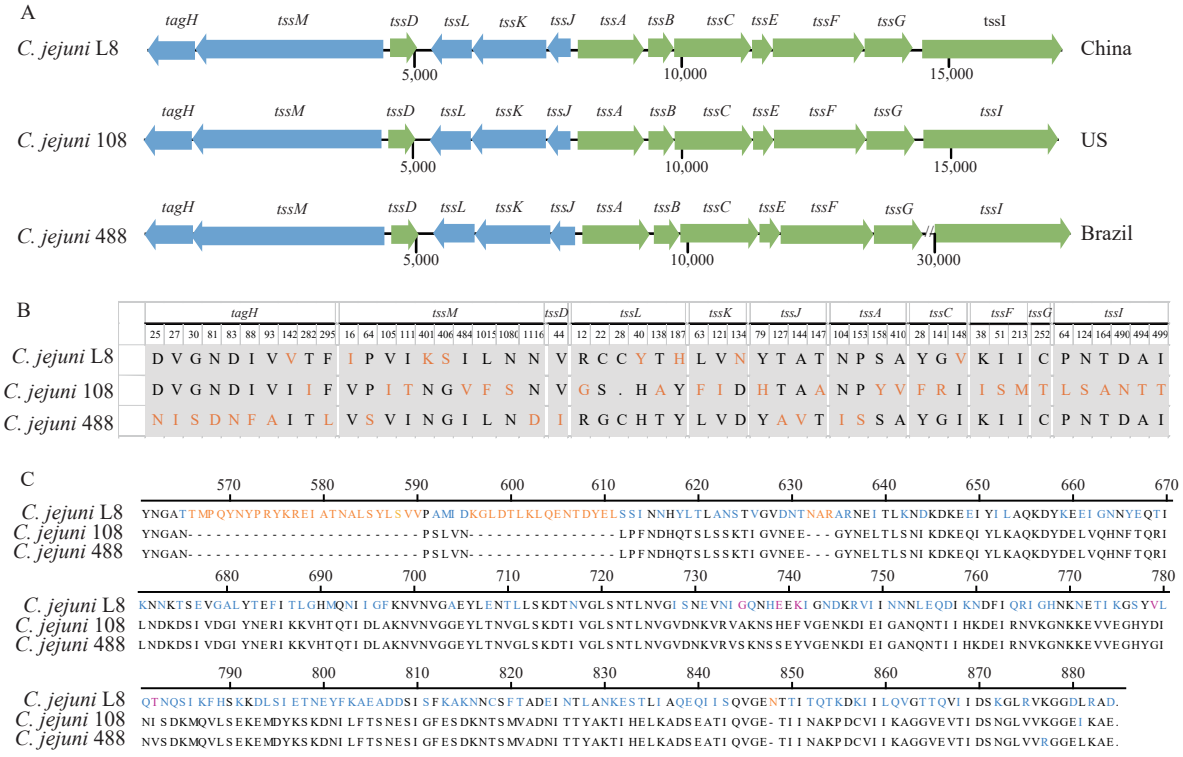

FIGURE 4. Comparison of 13 T6SS core components among L8, 108, and 488. (A) Organization of T6SS genes encoded by *C. jejuni* L8, 108, and 488. (B) Alignment of amino acid sequences of 11 genes. (C) Alignment of the amino acid sequence of TssI (VgrG) from the three *C. jejuni* strains after 560.
Note: The sequence alignment of TssI (VgrG) was truncated at 560. There was no change in the sequence alignment of TssB and TssE. Insertion sequences only in L8 are highlighted orange, and variant sequences are highlighted blue compared with the other two strains.

multiple consecutive or scattered mutations were present in L8's C-terminal VgrG, a crucial effector of the conserved T6SS. In the search for specific virulence factors, we found that L8 contained the complete CDT gene, with CdtA showing significant differences from those in other strains.

In bacterial infections, a crucial virulence determinant is the T6SS, which forms a nano-crossbow-like structure in the attacker cell's cytoplasm that propels an arrow composed of a haemolysin co-regulated protein tube and a VgrG spike to puncture the prey's cell wall (*4*). VgrG is an essential and conserved structural component in all reported T6SSs to date (*5*–*6*), and the C terminus of VgrG is widely conserved and necessary for functional T6SS assembly (*5*). Surprisingly, L8's C-terminal VgrG domain exhibited significant changes from positions 561 to 884, including the insertion of two long fragments and multiple consecutive or scattered mutations on their exterior. These alterations are very rare in previously reported T6SS structures (*3*). In contrast, the amino acid sequences between positions 108 and 488 showed 99.38% consistency. We hypothesize that this C-terminal VgrG domain was likely transformed into a toxin protein that may be associated with the patient's clinical phenotype. Notably, this study did not elucidate the specific role of this unique structure in VgrG function. Nevertheless, this finding implies that this unusual VgrG structure may enhance the initial impact of T6SS on bacterial antagonism, subversion of host cells, and niche colonization, raising the possibility that the injection of toxin proteins into host cells led to high fever and convulsions in the child.

Comparative analysis of genes within the T6SS core components showed greater similarities between L8 and 108 for *tagH*, *tssD*, and *tssA*, while L8 and 488 were more similar for *tssM*, *tssK*, *tssC*, *tssF*, *tssG*, and *tssI* (<500). Multiple scattered single amino acid mutations identified within the T6SS core components of each strain indicate individual divergences. These findings suggest that these genes warrant further investigation to elucidate T6SS function.

Although L8 and NCTC 11168 exhibited high similarity in the distribution of common virulence genes, their clinical phenotypes differed significantly. Unfortunately, no specific virulence factors were

identified in L8, unlike the potential virulence factors clearly observed in 81-176. However, phylogenetic analysis revealed that the subunit CdtA of CDT in L8 formed a distinct branch, indicating that its amino acid sequences were highly divergent from those of the other 66 strains. The toxic effects of CDT are primarily reflected in its ability to induce cell death and regulate the inflammatory response in human epithelial cells. *C. jejuni* CDT comprises three subunits: CdtA, CdtB, and CdtC. CdtA and CdtC bind to membrane lipid rafts, a crucial step for CdtB entry into cells (*7*). We hypothesize that the binding of CdtA variants and CdtC to membrane lipid rafts may facilitate CdtB entry into cells, potentially enhancing apoptosis and inflammation. Consequently, this series of processes likely exacerbated the patient's clinical presentation, although further functional verification is required.

The sequence type of L8 was ST-464, assigned to BAPS cluster 1, where 25 of the 26 genomes originated from either chickens (17 genomes) or humans (8 genomes), with one exception isolated from a farm (Figure 1B). This suggests the patient was likely infected by a chicken, a conclusion supported by epidemiological investigation. The child had come into contact with chicken feces on his mouth due to thrush treatment using a folk remedy. The patient was initially admitted on acyclovir and then switched to cefoperazone/sulbactam a week later, and was discharged after another week. Interestingly, a similar case was reported in China, where a strain isolated from the blood of a child with bacteremia was initially identified as "*Francisella*" by the automatic bacterial identification instrument VITEK2.0, later confirmed as *C. jejuni*. Another case clinically suspected as tularemia was later identified as *Paenibacillus assamensis* (*8*). These instances underscore the unreliability of depending solely on automatic bacterial identification instruments for accurate strain identification. Additionally, a case of bloodstream infection by *C. jejuni* was reported in Guizhou Province, in which the patient presented with syncope and high fever without diarrhea (*9*).

This work might expand our understanding of the clinical manifestations of campylobacteriosis. Furthermore, we recommend considering the potential significance of T6SS in the pathogenesis of *C. jejuni* when studying the genetic characterization of clinical phenotypes (*10*).

Conflicts of interest: No conflicts of interest.

Acknowledgements: the CDC workers who participated in the field epidemiological investigation and the doctors of Luxi County People's Hospital who treated the patient.

Funding: Supported by the National Natural Science Foundation of China (Grant No. 81874275 and 82102390) and the Natural Science Foundation of Beijing Municipality (Grant No. 7242188).

doi: 10.46234/ccdcw2024.182

Corresponding author: Yanhua Wang, wangyanhua@icdc.cn.

[1] Ecological Medicine Research Center, National Key Laboratory of Intelligent Tracking and Forecasting for Infectious Diseases, National Institute for Communicable Disease Control and Prevention, Chinese Center for Disease Control and Prevention, Beijing, China; [2] Department of Zoonotic Disease Control and Prevention, Yunnan Institute of Endemic Diseases Control & Prevention, Dali Bai Autonomous Prefecture, Yunnan Province, China; [3] Medical Laboratory Department, Yunnan Luxi County People's Hospital, Honghe Hani-Yi Autonomous Prefecture, Yunnan Province, China.

Submitted: February 18, 2024; Accepted: August 05, 2024

REFERENCES

1. Kaakoush NO, Castaño-Rodríguez N, Mitchell HM, Man SM. Global epidemiology of *Campylobacter* infection. Clin Microbiol Rev 2015;28(3):687 – 720. https://doi.org/10.1128/cmr.00006-15.
2. Chen HH, Dai YX, Chen JC, Zhang YY, Zhan L, Mei LL, et al. Epidemiological and whole genomic sequencing analysis of a *Campylobacter jejuni* outbreak in Zhejiang Province, China, May 2019. Foodborne Pathog Dis 2020;17(12):775 – 81. https://doi.org/10.1089/fpd.2020.2794.
3. Robinson L, Liaw J, Omole Z, Xia D, van Vliet AHM, Corcionivoschi N, et al. Bioinformatic analysis of the *Campylobacter jejuni* type VI secretion system and effector prediction. Front Microbiol 2021;12:694824. https://doi.org/10.3389/fmicb.2021.694824.
4. Durand E, Nguyen VS, Zoued A, Logger L, Péhau-Arnaudet G, Aschtgen MS, et al. Biogenesis and structure of a type VI secretion membrane core complex. Nature 2015;523(7562):555 – 60. https://doi.org/10.1038/nature14667.
5. Lopez J, Ly PM, Feldman MF. The tip of the VgrG spike is essential to functional type VI secretion system assembly in *Acinetobacter baumannii*. mBio 2020;11(1):e02761 – 19. https://doi.org/10.1128/mbio.02761-19.
6. Liang XY, Pei TT, Li H, Zheng HY, Luo H, Cui Y, et al. VgrG-dependent effectors and chaperones modulate the assembly of the type VI secretion system. PLoS Pathog 2021;17(12):e1010116. https://doi.org/10.1371/journal.ppat.1010116.
7. Yeh JY, Lin HJ, Kuo CJ, Feng CL, Chou CH, Lin CD, et al. *Campylobacter jejuni* cytolethal distending toxin C exploits lipid rafts to mitigate *Helicobacter pylori*-induced pathogenesis. Front Cell Dev Biol 2021;8:617419. https://doi.org/10.3389/fcell.2020.617419.
8. Zhang EM, Lu HC, Liu QH, Tang ZG, Li DJ, Jiang L, et al. *Paenibacillus assamensis* in joint fluid of man with suspected tularemia, China. Emerg Infect Dis 2018;24(8):1589 – 91. https://doi.org/10.3201/eid2408.180260.
9. Xiong LJ, Guo J. A case of bloodstream infection caused by *Campylobacter jejuni*. J Microbes Infect 2023;18(2):97 – 101. https://doi.org/10.3969/j.issn.1673-6184.2023.02.005.
10. Katz A, Porte L, Weitzel T, Varela C, Muñoz-Rehbein C, Ugalde JA, et al. Whole-genome sequencing reveals changes in genomic diversity and distinctive repertoires of T3SS and T6SS effector candidates in Chilean clinical *Campylobacter* strains. Front Cell Infect Microbiol 2023;13:1208825. https://doi.org/10.3389/fcimb.2023.1208825.

SUPPLEMENTARY MATERIAL

SUPPLEMENTARY TABLE S1. Specific ninety genes in *C. jejuni* L8 chromosome compared with NCTC 11168.

Start	End	Orientation	Gene name	Predicted function
940127	940471	+	L8GL000983	Hypothetical protein
940522	940968	−	L8GL000984	Recombinase XerC
940977	941459	−	L8GL000985	Recombinase XerC
941620	941850	+	L8GL000986	Mobilization protein
942097	942213	−	L8GL000987	Hypothetical protein
942404	942547	−	L8GL000988	Hypothetical protein
942559	942690	−	L8GL000989	Hypothetical protein
943032	943181	−	L8GL000990	Hypothetical protein
943453	943680	+	L8GL000991	Hypothetical protein
943961	944083	+	L8GL000992	Hypothetical protein
944059	944196	+	L8GL000993	Hypothetical protein
944217	944375	−	L8GL000994	Hypothetical protein
944447	944743	−	L8GL000996	Hypothetical protein
944745	944921	−	L8GL000995	Hypothetical protein
944937	945149	−	L8GL000997	Hypothetical protein
945333	945791	−	L8GL000998	Hypothetical protein
945845	947050	−	L8GL000999	Conjugal transfer protein TraG
947966	948769	−	L8GL001000	Hypothetical protein
948823	950124	−	L8GL001001	Hypothetical protein
950136	951584	−	L8GL001002	Hypothetical protein
951638	953605	−	L8GL001003	Hypothetical protein
953602	955536	−	L8GL001004	lipase family protein
955599	956096	−	L8GL001005	Hypothetical protein
956097	956228	−	L8GL001006	Uncharacterized protein
956215	956718	−	L8GL001007	Uncharacterized protein
956719	958251	−	L8GL001008	Hypothetical protein
958393	958710	−	L8GL001009	Uncharacterized protein
958718	960241	−	L8GL001010	Hypothetical protein
960256	960372	−	L8GL001011	Hypothetical protein
960498	960890	−	L8GL001012	Hypothetical protein
960887	961354	−	L8GL001013	Hypothetical protein
961424	962416	−	L8GL001014	Hypothetical protein
962908	963492	+	L8GL001015	Lysozyme
963521	963880	+	L8GL001016	Uncharacterized protein
964147	968079	+	L8GL001017	Hypothetical protein
968098	969366	+	L8GL001018	Hypothetical protein
969420	970223	+	L8GL001019	Hypothetical protein
971204	972076	+	L8GL001020	Hypothetical protein
972073	972486	+	L8GL001021	DNA-binding protein
972901	973275	+	L8GL001022	Hypothetical protein

Continued

Start	End	Orientation	Gene name	Predicted function
973358	974590	+	L8GL001023	Hypothetical protein
974749	974931	+	L8GL001024	Hypothetical protein
975105	975689	−	L8GL001025	Hypothetical protein
976064	976177	+	L8GL001026	Hypothetical protein
976181	976690	+	L8GL001027	Methyltransferase
976684	977322	+	L8GL001028	Hypothetical protein
977367	981617	+	L8GL001029	lipase family protein
981607	982353	+	L8GL001030	Hypothetical protein
982398	986330	+	L8GL001031	Hypothetical protein
986349	987617	+	L8GL001032	Hypothetical protein
987621	988520	−	L8GL001033	Hypothetical protein
988517	992044	−	L8GL001034	Hypothetical protein
992162	992677	+	L8GL001035	Hcp protein
992927	993700	−	L8GL001036	Asp/Glu-ADT subunit B
993697	995094	−	L8GL001037	Type VI secretion protein
995104	995550	−	L8GL001038	Type VI secretion protein
995676	996923	+	L8GL001039	Nucleobase: cation symporter
996992	997477	+	L8GL001040	Type VI secretion protein
997479	998933	+	L8GL001041	Type VI secretion protein
998936	999328	+	L8GL001042	Tgh104
999325	1001046	+	L8GL001043	Type VI secretion protein
1001043	1001951	+	L8GL001044	type VI secretion protein
1002120	1004753	+	L8GL001045	Type VI secretion protein VgrG
1004807	1005760	+	L8GL001046	Hypothetical protein
1005753	1007375	+	L8GL001047	Hypothetical protein
1007386	1008324	+	L8GL001048	Hypothetical protein
1008370	1008834	+	L8GL001049	Uncharacterized protein
1008831	1010081	+	L8GL001050	Hypothetical protein
1010074	1011165	+	L8GL001051	Hypothetical protein
1011179	1011733	+	L8GL001052	Hypothetical protein
1011788	1012741	+	L8GL001053	Hypothetical protein
1012731	1013117	+	L8GL001054	Hypothetical protein
1013132	1013689	+	L8GL001055	Tgh121
1013744	1014520	+	L8GL001056	Hypothetical protein
1014538	1015086	+	L8GL001057	Hypothetical protein
1015171	1015521	+	L8GL001058	Hypothetical protein
1015521	1016153	+	L8GL001059	Hypothetical protein
1016315	1018813	+	L8GL001060	type VI secretion protein VgrG
1018813	1020804	+	L8GL001061	Hypothetical protein
1020806	1021417	+	L8GL001062	Hypothetical protein
1022163	1022942	+	L8GL001063	Hypothetical protein
1022998	1025274	+	L8GL001064	Hypothetical protein

Continued

Start	End	Orientation	Gene name	Predicted function
1025241	1025471	+	L8GL001065	Hypothetical protein
1025625	1026233	+	L8GL001066	VgrG protein
1026292	1027011	+	L8GL001067	Hypothetical protein
1026995	1027168	+	L8GL001068	Hypothetical protein
1027184	1028044	+	L8GL001069	Uncharacterized protein
1028032	1029984	+	L8GL001070	Hypothetical protein
1029977	1031224	+	L8GL001071	Hypothetical protein
1031226	1032473	+	L8GL001072	Hypothetical protein

SUPPLEMENTARY TABLE S2. Basic information, BAPS clusters, and sequence types of 84 *C. jejuni* strains.

Strain	BAPS	Sequence type	Location	Host	Collection year
NCTC 11168	2	43	UK	Human blood	1981
81-176	3	604	USA	Human blood	1981
L8	1	464	Yunnan, China	Human blood	2018
2016-IZSVE-19-111250	2	50	Italy	Human feces	2016
R19.1007	1	–	Taiwan, China	Human feces	2019
NCTC11351	4	403	Belgium	Unknown	1980
BC	5	–	Guangzhou, China	Chicken	2016
CC19PF065	5	–	Fujian, China	Human feces	2019
C57	1	2140	Henan, China	Chicken	2018
C220	1	2140	Henan, China	Chicken	2018
C219	1	2140	Henan, China	Chicken	2018
C34	1	2140	Henan, China	Chicken	2018
C197	1	2140	Henan, China	Chicken	2018
C41	1	2140	Henan, China	Chicken	2018
C201	2	10075	Henan, China	Chicken	2018
C203	2	10075	Henan, China	Chicken	2018
C109	1	305	Henan, China	Chicken	2018
C1922C72	5	10086	Henan, China	Chicken	2019
ZS004	5	–	Zhejiang, China	Duck	2019
ZS005	5	–	Zhejiang, China	Duck	2019
ZS007	5	–	Zhejiang, China	Duck	2019
ZH003	5	10086	Zhejiang, China	Chicken	2018
ZH006	5	10086	Zhejiang, China	Chicken	2018
ZJB021	5	–	Zhejiang, China	Chicken	2018
ZJB020	5	–	Zhejiang, China	Chicken	2018
ZJB023	5	–	Zhejiang, China	Chicken	2018
ZS006	5	10086	Zhejiang, China	Duck	2019
CAMSA2002	2	21	Denmark	Chicken	2008
CAMSA2038	2	21	Denmark	Chicken	2008
CJ018CCUA	1	1972	Finland	Human blood	2002
CJ071CC464	1	3140	Finland	Human blood	1999
CJ067CC45	6	137	Finland	Human blood	2000

Continued

Strain	BAPS	Sequence type	Location	Host	Collection year
CJ074CC443	1	5671	Finland	Human blood	1998
CJ017CCUA	4	5673	Finland	human blood	2001
CJ066CC508	4		Finland	Human blood	2000
CJ515CC45	6	45	Finland	Human feces	2006
CJ031CC45	6	230	Finland	Human blood	1999
CJ088CC52	1	52	Finland	Human blood	2000
CJ090CC1332	5	1332	Finland	Human blood	2001
BfR-CA-14430	2	44	Germany	Chicken	2016
RM1510	3	22	Japan	Human blood	Unknown
RM3147	3	22	Mexico	Human blood	Unknown
GB03	3	22	Netherlands	Human blood	1995
GB28	3	660	Netherlands	Human blood	1999
RM3194	1	1471	South Africa	Human feces	1994
FORC_083	1	6849	Republic of Korea	Chicken	2017
FORC_046	3	22	Republic of Korea	Human feces	2016
1	1	464	Sweden	Chicken	Unknown
R18.1301	1	5	Taiwan, China	Human feces	2018
R16.2162	2	–	Taiwan, China	Human feces	2016
R16.0174	2	760	Taiwan, China	Human feces	2016
R16.4752	2	760	Taiwan, China	Human feces	2016
CFSAN054107	1	6238	Thailand	Unknown	2014
HF5-4A-4	2	861	UK	Farm	2012
NS4-5-1	2	21	UK	Farm	2012
NCTC12658	2	50	UK	Unknown	Unknown
HF5-7-1	6	45	UK	Farm	2012
CJM1cam	6	137	UK	Human blood	Unknown
NCTC12851	6	45	UK	Chicken	1993
NCTC 12664	2	50	UK	Chicken	1992
NCTC 12661	4	5843	UK	Avian	1992
12567	2	53	UK	Chicken	2005
NCTC 12660	2	21	UK	Chicken	1992
RM1221	1	354	USA	Chicken	2000
F	1	1212	USA	Chicken	2009
YH003	1	353	USA	Chicken	2014
CFSAN032806	2	222	USA	Chicken	2012
FJ3124	1	–	USA	Chicken	2009
FDAARGOS_422	2	883	USA	Human blood	Unknown
OD267	2	50	USA	Chicken	2009
R4B202	3	42	USA	Field Isolate	1983
RM1285	2	50	USA	Chicken	1997
RM1246-ERRC	6	45	USA	Human blood	Unknown
RM1245	3	22	USA	Human blood	1996
RM1477	3	22	USA	Human blood	1983

Continued

Strain	BAPS	Sequence type	Location	Host	Collection year
D33a	3	459	USA	Chicken	2003
A9a	1	2827	USA	Chicken	2003
YH002	2		USA	Chicken	2014
TS1218	1	607	USA	Chicken	2009
YQ2210	1	1212	USA	Chicken	2009
IF1100	1	462	USA	Chicken	2009
FDAARGOS_265	2	48	USA	Human blood	Unknown
FDAARGOS_263	2	43	USA	Human feces	1977
FDAARGOS_266	6	583	USA	ATCC strain	Unknown

Note: "–" means none

Review

A Review of the Latest Control Strategies for Mosquito-Borne Diseases

Jing Ni[1,&]; Jinna Wang[2,&]; Chunfu Fang[3,&]; Wenrong Zhang[1]; Zhenyu Gong[2,#]

ABSTRACT

Mosquito-borne diseases are persistent and potentially severe posing a threat to global pandemic preparedness. The risk of mosquito-borne virus transmission is rapidly increasing due to the unprecedented spread of viruses such as dengue and chikungunya, the disruption of global mosquito-borne disease control efforts following the emergence of coronavirus diseases 2019 (COVID-19) in 2019, global warming, and human activities. To address this global challenge, various innovative mosquito control technologies are being developed worldwide. This paper summarizes the latest advances in mosquito vector control, focusing on China's latest mosquito control strategies, to provide insights into implementing novel mosquito-borne disease control measures.

Global Overview of Mosquito-Borne Disease and Progress in Prevention and Control

In recent years, the global situation of mosquito-borne diseases has become increasingly severe with accelerated global urbanization and a growing population. According to the latest report of the World Health Organization (WHO), vector-borne diseases account for more than 17% of all infectious diseases and cause more than 700,000 deaths annually (*1*). Approximately 80% of the global population is at risk of contracting these diseases, making them a persistent public health problem (*2*). The two main types of mosquito-borne diseases currently prevalent are viral and parasitic diseases. Taking several priority mosquito-borne diseases as examples: in terms of vaccine development, no vaccines have been developed or are still in the experimental stage for chikungunya fever (*3*) and malaria (*4*). It is worth mentioning that the R21 malaria vaccine has shown excellent clinical efficacy and is expected to produce 100 million doses in 2024 and up to 200 million doses per year thereafter, which may outstrip demand in Africa in the future (*5*). The vaccine for yellow fever (*6*) has been developed but is not widely available in poorer parts of the world. Dengue fever has only two vaccines commercially available: Dengvaxia for those with a previous history of dengue and TAK-003 (*7*), which was approved by the WHO in 2023 for use in children aged 6–16 years in highly endemic areas. Butantan-DV (*8*), which will complete a five-year trial at the end of 2024, is not commercially available. In terms of endemic regions, dengue fever is endemic in 129 countries, with Asia accounting for nearly 70% of the global dengue case burden (*8*). Yellow fever has irregular outbreaks in Africa and the Americas (*6*), and chikungunya fever is currently present in more than 100 countries or territories around the globe, causing about 1 million infections per year (*9*). During the COVID-19 pandemic, malaria caused 63,000 deaths (*8*). Additionally, resistance to antimalarials is increasing, and a new generation of antimalarials and vaccines is urgently needed (*10*).

Among the malaria control measures already in place, long-lasting insecticidal nets (LLINs) (*11*) and indoor residual spraying (IRS) (*12*) are most commonly used. The recent COVID-19 pandemic has created a need for the R&D of new control tools, especially those that are less labor-intensive, simple, and effective to implement (*13*). In2Care® EaveTubes (ETs) (*13*) are inexpensive, innovative, and resistant vector control products that use heat and odor generated by natural air currents in ventilation ducts located under the eaves of a house to attract mosquitoes to insecticide-treated bed nets inside the ducts. New mosquito control methods are also emerging. Genetic sequencing methods can be used to control mosquito-borne diseases (*14*), by predicting the transmission routes of viruses carried by mosquitoes and the genetic characteristics of mosquitoes to enhance species surveillance. Ivermectin (*15*) is another potential tool, with an anti-mosquito effect in clinical trials that far exceeded *in vitro* laboratory experiment

predictions (*16*). Additionally, gene-driven technology utilizing *Wolbachia* has been applied in mosquito population suppression and modification (*17*) and appears to have some success; however, the implementation of this approach still requires long-term field experiments.

Global Mosquito Control Strategies and Challenges

Integrated Management

The strong adaptability of mosquitoes reduces the effectiveness of single vector control measures, contributing to the increasing prevalence of mosquito-borne diseases such as malaria, dengue fever, and yellow fever (*18*). Consequently, the WHO proposed the concept of integrated management in 2004 (*19*). Currently, integrated management is primarily implemented through two major aspects: technology and advocacy. Technological approaches include the timely diagnosis of mosquito-borne diseases (*20*), improved entomological testing (*21*), practical new mosquito traps for surveillance, the use of geographic information systems (GIS) for surveillance (*22*), and the use of new technologies to control mosquitoes and prevent transmission (e.g., deciphering the vectorial capacity of local mosquito populations and releasing improved mosquitoes) (*23*). Advocacy-level approaches include social mobilization, multi-sectoral joint mosquito control, and revision of mosquito control-related laws (*24*). However, the implementation of integrated management faces several challenges, such as mosquito control and ecological adaptability, uneven resources and capacity in different areas, and varying infrastructures and backgrounds of communities, necessitating time for comprehensive promotion (*25*).

Sustainable Mosquito Control

The sustainable mosquito vector control strategy was first mentioned in the WHO's Global Technical Strategy for Malaria 2016–2030 (*19*), and various countries have since taken different measures to implement this strategy.

In China, Qiyong Liu proposed the "sustainable vector strategy" (*26*), and academician Jianguo Xu suggested the "reverse pathogenesis" approach (*27*). The concept of "sustainable control" is characterized by health, economic, and ecological considerations, with multi-sectoral cooperation in vector biomonitoring, disease risk assessment, and control planning based on monitoring results, followed by a call for universal participation. "Reverse pathogenesis" aims to establish a forward-looking, proactive defense plan and joint prevention of major infectious diseases (*28*).

Policies adopted abroad primarily target both humans and mosquito vectors. Human-focused measures, known as human-mosquito interaction-social mobilization (*29*), emphasize identifying viruses with the potential for international transmission (*30*). Human-mosquito interaction is facilitated through online platforms, such as mobile communication technology and digital platforms, to share insect data (*31*). This approach broadens participation in mosquito vector prevention and control efforts. Subsequent offline mosquito disease prevention and control counseling workshops (*32*) further enhance residents' interest in and knowledge of mosquito vector control. Mosquito-targeted measures include utilizing biopesticides (*33*), employing insect sterility techniques (*34*) to genetically modify mosquitoes for post-release purposes, and developing artificial liquid diets without blood (*35*). These biological control methods offer a more environmentally friendly approach to mosquito control without jeopardizing non-target beneficial insect populations.

However, implementing these measures still requires time and effort because many communities are strongly skeptical about the purpose of releasing genetically modified mosquitoes and are concerned about potential negative impacts (*36*). Therefore, human-mosquito interactions require greater involvement from local communities and other stakeholders (*36*). Although genetically modified mosquitoes can help control mosquito-borne diseases such as malaria, they are not yet globally available (*37*). Additionally, while many methods effectively target parasites or viruses in mosquitoes, they can also disrupt or alter mosquito physiology, leading to changes in longevity, reproduction, and immunity (*38*). Therefore, the robustness and durability of transgenics remain debatable (*25*). Currently, some countries or regions also face dilemmas in adopting sustainable mosquito vector control measures (*39*), such as a lack of funding (*40*) and insufficient local expertise in mosquito species identification (*29*), leading to uneven global progress in sustainable mosquito vector control.

Global Vector Control Response 2017–2030

The WHO issued the Global Vector Control

Response 2017–2030 (GVCR) (*41*) on 2 October 2017 to combat vectors and vector-borne diseases (VBDs). By 2030, the GVCR aims to reduce mortality caused by VBDs by at least 75% and case incidence by at least 60% compared to 2016 levels, as well as to prevent VBD epidemics globally. Its key measures — strengthening inter- and intra-sectoral action and collaboration, engaging and mobilizing communities, enhancing vector surveillance, and scaling up and integrating tools and approaches — are comprehensively reflected in the integrated governance and sustainable control strategies of each country discussed above.

One Health Concept

One Health (OH) is an integrated, unifying approach to human and animal health, environmental health, food safety, and agricultural production (*42*), and its main applications in the field of mosquito-borne diseases are diagnostics for human treatment and mosquito diagnostics for vector control, which constitute two aspects of a broad and integrated ecosystem (*43*). A recent WHO article emphasizes the need to prioritize the inclusion of OH in strategic planning on the international political agenda (*44*), underscoring the importance of the OH concept.

Strategies for the Prevention and Control of Mosquito-borne Diseases in China, Focusing on Mosquito-free Villages

Vector control is a priority of the patriotic health campaign because it can effectively reduce disease spread, improve quality of life, and enhance living environments (*45*). In 2016, Zhejiang Province pioneered the development of "Mosquito-Free Villages" to address the persistence of mosquito-borne diseases (*46–47*).

The core concept of the Mosquito-Free Village is sustainable breeding ground control, with the innovation of integrating health into the government's "Ten Million Project", also known as "Beautiful Village Development" (*48*). For example, in Pujiang County (*49*) and Qingtian County (*50*), two demonstration counties, mosquito trapping lamps and *BI* were used in Pujiang County (*51*). In Qingtian County, the larval mosquito suction tube method and the double-layer stacked tent method were used for mosquito surveillance, transforming the rural ecological environment. Qingtian County also used a combination of government promotion and the introduction of the Patriotic Health Campaign Committee Office (PHCCO) to increase public recognition of Mosquito-Free Village construction. This was achieved through Party Day themes to increase the publicity of Mosquito-Free Village branding and adopt a low-cost and effective method to create a path toward environmental, mosquito vector disease, and human health improvement.

The corresponding construction standards have been issued and are available as models for other regions. On December 27, 2019, the local standard "Mosquito-Free Village" (DB3311/T 122-2019) was introduced, and on February 1, 2024, after continuous improvement and innovation, the group standard (T/ZJPCA 001-2024) "Guidelines for Sustainable Control of Countryside Vector Organisms — Four Pests" was officially released and implemented. Mosquito-Free Villages were subsequently promoted in all counties of Zhejiang Province; in Changsha, Hunan Province, in 2022; and in Xiangfeng Village, Fuling, Chongqing, in July 2023, marking the first pilot in Southwest China. These examples demonstrate that Mosquito-Free Villages are a cost-effective environmental remediation practice for sustainable mosquito vector control and a curative measure for realizing the WHO 2017–2030 strategy, which can be replicated and promoted. While the primary economic benefits of Mosquito-Free Villages vary, China is also conducting small-scale pilot programs using the *Wolbachia* mosquito sterilization method, with the expectation of national promotion in the future (*52*).

CONCLUSION

In short, mosquito control requires sustained efforts with three specific measures. First, each region should strengthen its monitoring system, train monitoring technicians, and establish a platform for sharing monitoring information to facilitate integrated early warning. Second, research should continue in the direction of biotechnology for mosquito control. Third, integrated environment-mosquito vector control should be carried out under the OH concept, as reflected in the construction of mosquito-free villages in China. With "mosquito-free" becoming the general direction and ultimate goal of prevention and control, it is the responsibility of every country to achieve a global "mosquito-free" world, using the goals of the "2017–2030 Global Vector Control Response" as a blueprint.

Conflicts of interest: No conflicts of interest.

doi: 10.46234/ccdcw2024.183

Corresponding author: Zhenyu Gong, zhygong@cdc.zj.cn.

[1] School of Public Health, Hangzhou Medical College, Hangzhou City, Zhejiang Province, China; [2] Department of Communicable Disease Control and Prevention, Zhejiang Provincial Center for Disease Control and Prevention, Hangzhou City, Zhejiang Province, China; [3] Quzhou Center for Disease Control and Prevention, Quzhou City, Zhejiang Province, China.
[&] Joint first authors.

Submitted: April 09, 2024; Accepted: August 03, 2024

REFERENCES

1. WHO. World malaria report 2022. 2022. https://www.who.int/teams/global-malaria-programme/reports/world-malaria-report-2022. [2023-12-14].
2. Engdahl CS, Tikhe CV, Dimopoulos G. Discovery of novel natural products for mosquito control. Parasit Vectors 2022;15(1):481. https://doi.org/10.1186/s13071-022-05594-z.
3. Cai L, Hu XY, Liu S, Wang L, Lu H, Tu H, et al. The research progress of Chikungunya fever. Front Public Health 2023;10:1095549. https://doi.org/10.3389/fpubh.2022.1095549.
4. Varo R, Chaccour C, Bassat Q. Update on malaria. Med Clin (Barc) 2020;155(9):395 – 402. https://doi.org/10.1016/j.medcli.2020.05.010.
5. Genton B. R21/Matrix-M^{TM} malaria vaccine: a new tool to achieve WHO's goal to eliminate malaria in 30 countries by 2030? J Travel Med 2023;30(8):taad140. http://dx.doi.org/10.1093/jtm/taad140.
6. Tuells J, Henao-Martínez AF, Franco-Paredes C. Yellow fever: a perennial threat. Arch Med Res 2022;53(7):649 – 57. https://doi.org/10.1016/j.arcmed.2022.10.005.
7. Biswal S, Borja-Tabora C, Martinez Vargas L, Velásquez H, Theresa Alera M, Sierra V, et al. Efficacy of a tetravalent dengue vaccine in healthy children aged 4-16 years: a randomised, placebo-controlled, phase 3 trial. Lancet 2020;395(10234):1423 – 33. https://doi.org/10.1016/S0140-6736(20)30414-1.
8. Bhatt S, Gething PW, Brady OJ, Messina JP, Farlow AW, Moyes CL, et al. The global distribution and burden of dengue. Nature 2013;496(7446):504 – 7. https://doi.org/10.1038/nature12060.
9. Zhang WR, Wang JN, Liu QM, Gong ZY. A review of pathogens transmitted by the container-inhabiting mosquitoes, aedes albopictus, a global public health threat. China CDC Wkly 2023;5(44):984 – 90. https://doi.org/10.46234/ccdcw2023.185.
10. Suh PF, Elanga-Ndille E, Tchouakui M, Sandeu MM, Tagne D, Wondji C, et al. Impact of insecticide resistance on malaria vector competence: a literature review. Malar J 2023;22(1):19. https://doi.org/10.1186/s12936-023-04444-2.
11. Karl S, Katusele M, Freeman TW, Moore SJ. Quality control of long-lasting insecticidal nets: are we neglecting it? Trends Parasitol 2021;37(7):610-21. http://dx.doi.org/10.1016/j.pt.2021.03.004.
12. Corrêa APSA, Galardo AKR, Lima LA, Câmara DCP, Müller JN, Barroso JFS, et al. Efficacy of insecticides used in indoor residual spraying for malaria control: an experimental trial on various surfaces in a "test house". Malar J 2019;18(1):345. https://doi.org/10.1186/s12936-019-2969-6.
13. N'Guessan R, Assi SB, Koffi A, Ahoua Alou PL, Mian A, Achee NL, et al. EaveTubes for control of vector-borne diseases in Côte d'Ivoire: study protocol for a cluster randomized controlled trial. Trials 2023;24(1):704. https://doi.org/10.1186/s13063-023-07639-9.
14. Kurucz K, Zeghbib S, Arnoldi D, Marini G, Manica M, Michelutti A, et al. *Aedes koreicus*, a vector on the rise: Pan-European genetic patterns, mitochondrial and draft genome sequencing. PLoS One 2022;17(8):e0269880. https://doi.org/10.1371/journal.pone.0269880.
15. Kobylinski KC, Tipthara P, Wamaket N, Chainarin S, Kullasakboonsri R, Sriwichai P, et al. Ivermectin metabolites reduce *Anopheles* survival. Sci Rep 2023;13(1):8131. https://doi.org/10.1038/s41598-023-34719-2.
16. Bhatt S, Weiss DJ, Cameron E, Bisanzio D, Mappin B, Dalrymple U, et al. The effect of malaria control on *Plasmodium falciparum* in Africa between 2000 and 2015. Nature 2015;526(7572):207 – 11. https://doi.org/10.1038/nature15535.
17. Wang GH, Gamez S, Raban RR, Marshall JM, Alphey L, Li M, et al. Combating mosquito-borne diseases using genetic control technologies. Nat Commun 2021;12(1):4388. https://doi.org/10.1038/s41467-021-24654-z.
18. Mafra-Neto A, Dekker T. Novel odor-based strategies for integrated management of vectors of disease. Curr Opin Insect Sci 2019;34:105 – 11. https://doi.org/10.1016/j.cois.2019.05.007.
19. WHO. Global technical strategy for malaria 2016–2030, 2021 update. 2021. https://www.who.int/publications-detail-redirect/9789240031357. [2023-12-14].
20. Manzi S, Nelli L, Fortuna C, Severini F, Toma L, Di Luca M, et al. A modified BG-Sentinel trap equipped with FTA card as a novel tool for mosquito-borne disease surveillance: a field test for *flavivirus* detection. Sci Rep 2023;13(1):12840. https://doi.org/10.1038/s41598-023-39857-1.
21. Sarma DK, Rathod L, Mishra S, Das D, Agarwal A, Sharma G, et al. Molecular surveillance of dengue virus in field-collected *Aedes* mosquitoes from Bhopal, central India: evidence of circulation of a new lineage of serotype 2. Front Microbiol 2023;14:1260812. https://doi.org/10.3389/fmicb.2023.1260812.
22. Paradkar PN, Sahasrabudhe PR, Ghag Sawant M, Mukherjee S, Blasdell KR. Towards integrated management of dengue in Mumbai. Viruses 2021;13(12):2436. https://doi.org/10.3390/v13122436.
23. Fouet C, Kamdem C. Integrated mosquito management: is precision control a luxury or necessity? Trends Parasitol 2019;35(1):85 – 95. http://dx.doi.org/10.1016/j.pt.2018.10.004.
24. Mulderij-Jansen V, Pundir P, Grillet ME, Lakiang T, Gerstenbluth I, Duits A, et al. Effectiveness of *Aedes*-borne infectious disease control in Latin America and the Caribbean region: A scoping review. PLoS One 2022;17(11):e0277038. https://doi.org/10.1371/journal.pone.0277038.
25. Adelman ZN, Kojin BB. Malaria-resistant mosquitoes (Diptera: Culicidae); The principle is proven, but will the effectors be effective? J Med Entomol 2021;58(5):1997-2005. http://dx.doi.org/10.1093/jme/tjab090.
26. Liu QY. The sustainable control strategy and key technology of Aedes vector. Electron J Emerg Infect Dis 2018;3(2):75 – 9. https://doi.org/10.19871/j.cnki.xfcrbzz.2018.02.004.
27. Liu QY, Liu XB, Chang N, Zhang L. Advances and achievements in the surveillance and control of vectors and vector-borne diseases in China, 2012-2021. Chin J Vector Biol Control 2022;33(5):613 – 21,654. https://doi.org/10.11853/j.issn.1003.8280.2022.05.001.
28. Xu JG. Reverse microbial etiology. Dis Surveill 2019;34(7):593 – 8. https://doi.org/10.3784/j.issn.1003-9961.2019.07.005.
29. Bartumeus F, Costa GB, Eritja R, Kelly AH, Finda M, Lezaun J, et al. Sustainable innovation in vector control requires strong partnerships with communities. PLoS Negl Trop Dis 2019;13(4):e0007204. https://doi.org/10.1371/journal.pntd.0007204.
30. Petrone ME, Earnest R, Lourenço J, Kraemer MUG, Paulino-Ramirez R, Grubaugh ND, et al. Asynchronicity of endemic and emerging mosquito-borne disease outbreaks in the Dominican Republic. Nat Commun 2021;12(1):151. https://doi.org/10.1038/s41467-020-20391-x.
31. Wang HM, Qiu JQ, Li C, Wan HL, Yang CH, Zhang T. Applying the spatial transmission network to the forecast of infectious diseases across multiple regions. Front Public Health 2022;10:774984. https://doi.org/10.3389/fpubh.2022.774984.
32. Aerts C, Revilla M, Duval L, Paaijmans K, Chandrabose J, Cox H, et al. Understanding the role of disease knowledge and risk perception in shaping preventive behavior for selected vector-borne diseases in Guyana. PLoS Negl Trop Dis 2020;14(4):e0008149. https://doi.org/10.1371/journal.pntd.0008149.

33. Isman MB. Botanical insecticides in the twenty-first century—fulfilling their promise? Annu Rev Entomol 2020;65:233-49. http://dx.doi.org/10.1146/annurev-ento-011019-025010.
34. Zheng XY, Zhang DJ, Li YJ, Yang C, Wu Y, Liang X, et al. Incompatible and sterile insect techniques combined eliminate mosquitoes. Nature 2019;572(7767):56 – 61. https://doi.org/10.1038/s41586-019-1407-9.
35. Sharma M, Kumar V. Mosquito-larvicidal Binary (BinA/B) proteins for mosquito control programs —advancements, challenges, and possibilities. Curr Res Insect Sci 2022;2:100028. https://doi.org/10.1016/j.cris.2021.100028.
36. Resnik DB. Two unresolved issues in community engagement for field trials of genetically modified mosquitoes. Pathog Glob Health 2019;113(5):238 – 45. https://doi.org/10.1080/20477724.2019.1670490.
37. Müller R, Bálint M, Hardes K, Hollert H, Klimpel S, Knorr E, et al. RNA interference to combat the Asian tiger mosquito in Europe: a pathway from design of an innovative vector control tool to its application. Biotechnol Adv 2023;66:108167. https://doi.org/10.1016/j.biotechadv.2023.108167.
38. Sabet A, Goddard J. Promise or peril: using genetically modified mosquitoes in the fight against vector-borne disease. Am J Med 2022;135(3):281 – 3. https://doi.org/10.1016/j.amjmed.2021.08.036.
39. Connelly R. Highlights of medical entomology 2018: the importance of sustainable surveillance of vectors and vector-borne pathogens. J Med Entomol 2019;56(5):1183 – 7. https://doi.org/10.1093/jme/tjz134.
40. Horstick O, Runge-Ranzinger S. Multisectoral approaches for the control of vector-borne diseases, with particular emphasis on dengue and housing. Trans Roy Soc Trop Med Hyg 2019;113(12):823 – 8. https://doi.org/10.1093/trstmh/trz020.
41. WHO. Global vector control response 2017-2030. 2017. https://www.who.int/publications-detail-redirect/9789241512978. [2023-12-14].
42. WHO. Tripartite and UNEP support OHHLEP's definition of "One Health". 2021. https://www.who.int/news/item/01-12-2021-tripartite-and-unep-support-ohhlep-s-definition-of-one-health. [2023-12-14].
43. Lorusso V. Parasitology and one health—perspectives on Africa and beyond. Pathogens 2021;10(11):1437. https://doi.org/10.3390/pathogens10111437.
44. WHO. Quadripartite call to action for One Health for a safer world. 2023. https://www.who.int/news/item/27-03-2023-quadripartite-call-to-action-for-one-health-for-a-safer-world. [2023-12-14].
45. Qi YP, Wang JN, Wu YY, Fu XF, Li YF, Huang J, et al. Evaluation and discussion of effect of "mosquito and fly-free village" establishment in Hongxi village, Jiashan, Zhejiang. Dis Surveill 2021;36(9):873 – 8. https://doi.org/10.3784/jbjc.202106010313.
46. Guo S, Huang WZ, Sun JM, Gong ZY, Ling F, Wu HZ, et al. "Mosquito-free villages": practice, exploration, and prospects of sustainable Mosquito Control - Zhejiang, China. China CDC Wkly 2019;1(5):70 – 4. https://doi.org/10.46234/ccdcw2019.021.
47. Guo S, Huang W, Ling F, Wu H, Sun J, Lou Y, et al. Discussion on construction standard and evaluation index of "mosquito-free village" in Zhejiang province. Chin J Vector Biol Control 2018;29(2):177 – 80. https://doi.org/10.11853/j.issn.1003.8280.2018.02.016.
48. Liu YS, Zhou Y. Challenges and countermeasures for beautiful countryside construction in China. J Agric Resour Environ 2015;32(2):97 – 105. https://doi.org/10.13254/j.jare.2015.0092.
49. Wu H, Liu Y, Huang W, Ling F, Lou YJ, Sun J, et al. Evaluation on construction of "mosquito-free village" in Pujiang county, Zhejiang, China. Chin J Vector Biol Control 2018;29(3):283 – 6. https://doi.org/10.11853/j.issn.1003.8280.2018.03.016.
50. Zhu HB, Ye HF, Chen M, Zeng Y, Chen F, Fu ZJ. Effectiveness evaluation of 'mosquito-free village' construction in Qingtian county, Zhejiang province, China. Chin J Vector Biol Control 2021;32(3):365 – 8. https://doi.org/10.11853/j.issn.1003.8280.2021.03.021.
51. State Administration for Market Regulation, Standardization Administration. GB/T 23797-2020 Surveillance methods for vector density—Mosquito. Beijing: Standards Press of China, 2020. http://www.csres.com/detail/354742.html. (In Chinese).
52. Zheng XY, Wu Y, Zhang DJ, Hong XY, Xi ZY. Combining Wolbachia-based approach and sterile insect techniques eliminate *Aedes albopictus* population in field. J Nanjing Agric Univ 2020;43(3):387 – 91. https://doi.org/10.7685/jnau.202003100.

Youth Editorial Board

Director Lei Zhou

Vice Directors Jue Liu Tiantian Li Tianmu Chen

Members of Youth Editorial Board

Jingwen Ai
Li Bai
Yuhai Bi
Yunlong Cao
Gong Cheng
Liangliang Cui
Meng Gao
Jie Gong
Yuehua Hu
Jia Huang
Xiang Huo
Xiaolin Jiang
Yu Ju
Min Kang
Huihui Kong
Lingcai Kong
Shengjie Lai
Fangfang Li
Jingxin Li
Huigang Liang
Di Liu
Jun Liu
Li Liu
Yang Liu
Chao Ma
Yang Pan
Zhixing Peng
Menbao Qian
Tian Qin
Shuhui Song
Kun Su
Song Tang
Bin Wang
Jingyuan Wang
Linghang Wang
Qihui Wang
Xiaoli Wang
Xin Wang
Feixue Wei
Yongyue Wei
Zhiqiang Wu
Meng Xiao
Tian Xiao
Wuxiang Xie
Lei Xu
Lin Yang
Canqing Yu
Lin Zeng
Yi Zhang
Yang Zhao
Hong Zhou

Indexed by Science Citation Index Expanded (SCIE), Social Sciences Citation Index (SSCI), PubMed Central (PMC), Scopus, Chinese Scientific and Technical Papers and Citations, and Chinese Science Citation Database (CSCD)

Copyright © 2024 by Chinese Center for Disease Control and Prevention

All Rights Reserved. No part of the publication may be reproduced, stored in a retrieval system, or transmitted in any form or by any means, electronic, mechanical, photocopying, recording, or otherwise without the prior permission of *CCDC Weekly*. Authors are required to grant *CCDC Weekly* an exclusive license to publish.

All material in *CCDC Weekly* Series is in the public domain and may be used and reprinted without permission; citation to source, however, is appreciated.

References to non-China-CDC sites on the Internet are provided as a service to *CCDC Weekly* readers and do not constitute or imply endorsement of these organizations or their programs by China CDC or National Health Commission of the People's Republic of China. China CDC is not responsible for the content of non-China-CDC sites.

The inauguration of *China CDC Weekly* is in part supported by Project for Enhancing International Impact of China STM Journals Category D (PIIJ2-D-04-(2018)) of China Association for Science and Technology (CAST).

CCDC weekly

Vol. 6 No. 33 Aug. 16, 2024

Responsible Authority
National Disease Control and Prevention Administration

Sponsor
Chinese Center for Disease Control and Prevention

Editing and Publishing
China CDC Weekly Editorial Office
No.155 Changbai Road, Changping District, Beijing, China
Tel: 86-10-63150501, 63150701
Email: weekly@chinacdc.cn

CSSN
ISSN 2096-7071 (Print)
ISSN 2096-3101 (Online)
CN 10-1629/R1